OFFICE OF CIVILIAN RADIOACTIVE WASTE MANAGEMENT
CALCULATION COVER SHEET

1. QA: QA
Page: 1 Of: 62

2. Calculation Title

EQ6 Calculation for Chemical Degradation of Shippingport LWBR (Th/U Oxide) Spent Nuclear Fuel Waste Packages

3. Document Identifier (including Revision Number)

CAL-EDC-MD-000008 REV 00

4. Total Attachments	5. Attachment Numbers – Number of pages in each
2	I-14, II (9 CDs)

	Print Name	Signature	Date
6. Originator	Sara Arthur	Sara Arthur (P.A.) 9/6/2000	9/6/2000
7. Checker	Patrick Brady	Pat Brady	9/6/2000
8. Lead	Peter Gottlieb	Peter Gottlieb	9/14/2000

9. Remarks

Revision History

10. Revision No.	11. Description of Revision
REV 00	Initial Issue

CONTENTS

FIGURES

Page

TABLES

Page

TABLES (Continued)

Page

1. PURPOSE

The Monitored Geologic Repository (MGR) Waste Package Department of the Civilian Radioactive Waste Management System Management & Operating contractor (CRWMS M&O) performed calculations to provide input for disposal of spent nuclear fuel (SNF) from the Shippingport Light Water Breeder Reactor (LWBR) (Ref. 1). The Shippingport LWBR SNF has been considered for disposal at the potential Yucca Mountain site. Because of the high content of fissile material in the SNF, the waste package (WP) design requires special consideration of the amount and placement of neutron absorbers and the possible loss of absorbers and SNF materials over geologic time. For some WPs, the outer shell corrosion-resistant material (CRM) and the corrosion-allowance inner shell may breach (Refs. 2 and 3), allowing the influx of water. Water in the WP will moderate neutrons, increasing the likelihood of a criticality event within the WP; and the water may, in time, gradually leach the fissile components and neutron absorbers from the WP, further affecting the neutronics of the system.

This study presents calculations of the long-term geochemical behavior of WPs containing a Shippingport LWBR SNF seed assembly, and high-level waste (HLW) glass canisters arranged according to the codisposal concept (Ref. 4). The specific study objectives were to determine:

1. The extent to which criticality control material, suggested for this WP design, will remain in the WP after corrosion/dissolution of the initial WP configuration (such that it can be effective in preventing criticality)

2. The extent to which fissile uranium and fertile thorium will be carried out of the degraded WP by infiltrating water (such that internal criticality is no longer possible, but the possibility of external criticality may be enhanced)

3. The nominal chemical composition for the criticality evaluations of the WP design, and to suggest the range of parametric variations for additional evaluations.

The scope of this calculation, the chemical compositions (and subsequent criticality evaluations), of the simulations are limited to time periods up to 3.17×10^5 years. This longer time frame is closer to the one million year time horizon recently recommended by the National Academy of Sciences to the Environmental Protection Agency for performance assessment related to a nuclear repository (Ref. 5). However, it is important to note that after 100,000 years, most of the materials of interest (fissile and absorber materials) will have either been removed from the WP, reached a steady state, or been transmuted.

The calculation included elements with high neutron-absorption cross sections, notably gadolinium (Gd), as well as the fissile materials. The results of this analysis will be used to ensure that the type and amount of criticality control material used in the WP design will prevent criticality.

This document has been prepared according to Administrative Procedure AP-3.12Q, *Calculations* (Ref. 50), and is subject to the Quality Assurance Requirements and Description (QARD)(Ref. 41). This calculation has been prepared in accordance with the development plan, *DOE SNF Analysis Plan for FY2000* (Ref. 51).

2. METHOD

The method used for this analysis involves the following steps:

- Use of basic EQ3/6 (software package, described in Section 4.1 and in Ref. 22) capability for tracing the progress of reactions with evolution of the chemistry, which includes the estimation of the concentrations remaining in solution and the composition of the precipitated solids. (EQ3 is used to determine a starting fluid composition for EQ6 calculations; it does not simulate reaction progress.)

- Evaluation of available data on the range of dissolution rates for the materials involved, to be used as material/species input for each time step.

- Use of "solid-centered flow-through" mode (SCFT) in EQ6; in this mode, an increment of aqueous "feed" solution is added continuously to the WP system, and a like volume of the existing solution is removed, simulating a continuously-stirred tank reactor. This mode is discussed in Section 4.

- Determination of fissile material concentrations in solution as a function of time (from the output of EQ6 simulated reaction times up to 3.17×10^5 years).

- Calculation of the amount of fissile material released from the WP as a function of time (fissile material loss reduces the chance of criticality within the WP).

- Determination of concentrations of neutron absorbers, such as Gd, in solution as a function of time (from the output of EQ6 over times up to 3.17×10^5 years).

- Calculation of the amounts of neutron absorbers retained within the WP as a function of time.

- Composition and amounts of solids (precipitated minerals or corrosion products, and unreacted WP materials).

The EQ3/6 calculations reported in this document used version 7.2b of the code, which is complete, mathematically correct and technically adequate for the application (Ref. 18). Further detail on the specific methods employed for each step is available in Section 5 of this calculation.

With regard to the development of this calculation, the control of the electronic management of data was evaluated in accordance with AP-SV.1Q, *Control of the Electronic Management of Information* (Ref. 52). The evaluation (Ref. 53) determined that current work processes and procedures are adequate for the control of electronic management of data for this activity.

3. ASSUMPTIONS

All assumptions are for preliminary design. All assumptions are used throughout Section 5.

3.1 The Enhanced Design Alternative (EDA) II waste package is assumed for Shippingport LWBR. The basis for this assumption is that the EDA II design superseded the Viability Assessment (VA) design shortly after the Shippingport LWBR calculations began.

3.2 It is assumed that an aqueous solution fills all voids within WPs, and that the solutions that drip into the WP will have the major ion composition of J-13 well water as given in Reference 60 (DTN: MO0006J13WTRCM.000), and the minor components in the solution as given in Reference 6 (DTN: LL980711104242.054) for at least 3.17×10^5 years. The basis for the first part of this assumption is that it provides the maximum degradation rate with the potential for the fastest flushing of the neutron absorber from the WP, and is thereby conservative. The basis for the second and third part of the assumption is that the groundwater composition is controlled largely by transport through the host rock, over pathways of hundreds of meters, and the host rock composition is not expected to change substantially over 10^6 years. For a few thousand years after waste emplacement, the composition may differ because of perturbations resulting from reactions with engineered materials and from the thermal pulse. These are not taken into account in this calculation because the CRM and corrosion allowance inner liner are not expected to breach until after that perturbed period. Therefore, the early perturbation is not relevant to the calculations reported in this document. See Assumption 3.3.

3.3 It is assumed that the density of J-13 well water is 1.0 g/cm^3. The basis of this assumption is that in dilute solutions, the density is extremely close to that for pure water and that any differences are insignificant in respect to other uncertainties in the data and calculations. Moreover, this number is used only initially in EQ3/6 to convert concentrations of dissolved substances from parts per million to molalities.

3.4 The assumption that the water entering the WP can be approximated by the J-13 well water implicitly assumes that any effects of contact with the drift liner will be minimal after a few thousand years. The basis for this assumption is the following: (A) The drift liner at the top of the drift is expected to collapse with the roof support well before 1000 years; and (B) the water flowing through the concrete liner, dominantly along fractures, will be in contact with the degradation products of the liner which will have come close to equilibrium with the water moving through the rock above the repository. Interaction of water in the fractures with any unaltered concrete between fractures would be minimal owing to the slow rate of diffusion through the matrix compared to rate of flow through fractures.

3.5 It is assumed that water may circulate freely enough in the partially degraded WP that all degraded solid products may react with each other through the aqueous solution medium.

The basis for this assumption is that this provides one bound for the extent of chemical interactions within the WP.

3.6 It is assumed that data in the 25°C thermodynamic database can be used for the calculation. The basis for this assumption is that though the initial breach of the WP may occur when the WP contents are at temperatures ≥ 50°C (Ref. 7, Figures 3-20 through 3-22), at times > 25,000 years, the WP temperatures are likely to be close to 25°C. Since the solubility of $GdPO_4$ is retrograde (Ref. 8) (i.e., decreases with increasing temperature), use of the lower-temperature database is likely to be conservative for the purposes of this calculation.

3.7 In general it is assumed that chromium and molybdenum will oxidize fully to chromate (or dichromate) and molybdate, respectively. This assumption is based on the available thermodynamic data, which indicate that in the presence of air, the chromium and molybdenum would both oxidize to the VI valence state. Laboratory observation of the corrosion of Cr and Mo containing steels and alloys, however, indicates that any such oxidation would be extremely slow. In fact, oxidation to the VI state may not occur at a significant rate with respect to the time frame of interest, or there may exist stable Cr(III) solids that substantially lower aqueous Cr concentration. For the present analyses, the assumption is made that, over the times of concern, oxidation will occur. This is conservative for times of several thousand years after WP breach, when the high pH solution from any drift liner effects will have been flushed out of the WP. Extreme acidification of the water will enhance solubility (Ref. 2) and transport of neutron absorber out of the WP, thereby separating it preferentially from fissile material.

3.8 It is assumed that the CRM (the outer shell) of the WP will react so slowly with the infiltrating water (and water already in the WP) as to have a negligible effect on the chemistry. The bases for these assumption consist of the facts that the CRM is fabricated from Alloy 22 (see nomenclature in Section 5.1.1), which corrodes very slowly compared (1) to other reactants in the WP, and (2) to the rate at which soluble corrosion products will likely be flushed from the WP.

3.9 Gases in the WP solution remain in equilibrium with the ambient atmosphere outside the WP. In other words, contact of WP fluids with the gas phase in the repository is envisioned to be sufficient to maintain equilibrium with the CO_2 and O_2 present, whether or not this is the normal atmosphere in open air or rock gas that seeps out of the adjacent tuff. Moreover, the specific partial pressures of CO_2 and O_2 of the ambient repository atmosphere are set to, respectively, $10^{-3.0}$ and $10^{-0.7}$ atm. The basis for the oxygen partial pressure is that it is equivalent to that in the atmosphere. The basis for choosing the carbon dioxide pressure was to reflect the observation that J-13 well water appears to be in equilibrium with above-atmospheric carbon dioxide levels (Ref. 9, Table 8; Ref. 10, p. F-210).

3.10 It is assumed that precipitated solids are deposited, remain in place, and are not mechanically eroded or entrained as colloids in the advected water. The basis for this assumption is that since dissolved fissile material (U, Th) may be adsorbed on colloids (clays, iron oxides) or may be precipitated as colloids during WP degradation (Ref. 7, Sec. 3.5 and 3.6) it is conservative, for internal criticality, to assume that all precipitated solids, including mobile colloids, will be deposited inside the WP rather than transported out of the WP.

3.11 It is assumed that corrosion rates will not be significantly enhanced by microbiologically influenced corrosion (MIC). The bases for this assumption are that: (1) MIC will probably not occur until the repository has cooled to temperatures below 100°C (212°F) and relative humidity is above 60%, (2) although MIC may increase corrosion pit and crevice density, its effect on corrosion rate will be low, and (3) Alloy 22 has not been associated with documented cases of MIC (Ref. 7, p 3-84).

3.12 It is assumed that sufficient decay heat is retained within the WP over times of interest to cause convective circulation and mixing of the water inside the WP. The analysis that serves as the basis for this assumption is discussed in Reference 11 (Attachment VI).

3.13 It is assumed that the reported alkalinity in analyses of J-13 well water corresponds to bicarbonate (HCO_3^-) alkalinity. Contributors to alkalinity in J-13 well water, in addition to bicarbonate, potentially include borate, phosphate, and silicate. However, at pH less than 9, the contribution of silicate will be small, and in any case the concentrations of all three of these components in J-13 well water are small. Fluoride or nitrate do not contribute to alkalinity unless a sufficiently low pH is reached. The basis for this assumption is the observation that the calculated electrical neutrality, using the assumption, is zero, within the analytical uncertainty, as it should be. The same assumption is implicitly made in Reference 60 (DTN: MO0006J13WTRCM.000).

3.14 It is assumed that the rate of entry of water into, as well as the rate of egress from, a WP is equal to the rate at which water drips onto the WP. The basis for this assumption is that for most of the time frame of interest, i.e., long after the corrosion barriers become largely degraded, it is more reasonable to assume that all or most of the water will enter the degraded WP than to assume that a significant portion will instead be diverted around the remains. Diversion of the water with a consequent lower entry rate has not been represented by the present calculations.

3.15 It is assumed that the most insoluble solids for a fissile radionuclide will form. This approach is conservative with respect to internal criticality since it will lead to the maximum retention of fissile material within the WP during EQ6 runs.

3.16 A number of minor assumptions have been made about the geometry of the Shippingport LWBR codisposal WP. The bases for these assumptions are outlined and referenced in the spreadsheets "doecan_EDA2.xls", "LWBRshapes.xls", "ShipLWBR.xls"

(Attachment II), Reference 12, and are also discussed in Section 5.1. These assumptions were used to represent the WP geometry with the greatest accuracy possible. Where inadequate information about WP geometry was available, or it was necessary to choose among competing representations of WP geometry, the choice that appeared to lead to the greatest conservatism was always chosen.

3.17 For any WP components that were described as "316" stainless steel, without indication of the carbon grade, the alloy was assumed to be the low-carbon equivalent (see Section 5.1.1 for nomenclature). The basis for this assumption is that, in general, the carbon in the steel is totally insignificant compared to the carbon supplied by the fixed CO_2 fugacity of the EQ3/6 calculation, and to the constant influx of carbonate via J-13 well water. An underestimation of carbon in steel results in a slight overestimation of the remaining metals in the steel, which increases acid production very slightly and is therefore conservative, since low pH may increase loss of Gd from the WP.

3.18 A published estimate of the density of AM-350 stainless steel could not be found. For the calculation, the density is taken to be 7.9 g/cm^3, a reasonable value on the high side based on the range exhibited by other stainless steels (Ref. 13, p. 360). The density of AM-350 stainless steel is needed to calculate the mass of the seed assembly grids. The mass of the grids is a small fraction of the overall mass of the seed assemblies. Therefore, the basis of this assumption is the observation that the induced error is negligible. A published estimate of the degradation rate of AM-350 stainless steel could not be found. For the calculation, the degradation rate was assumed to be the same as the degradation rate of 316L stainless steel. The basis for this assumption is that AM-350 and 316L stainless steel are very similar in composition (See Table 1) and are therefore likely to have a similar degradation rate.

3.19 The Inconel X-750, Inconel 600, and Zircaloy-4 in the LWBR fuel rods and assemblies are assumed inert. The basis for this assumption is that these materials have low chemical reactivities at low temperatures.

3.20 Zircaloy and Zr corrosion kinetics studies (Ref. 14) revealed these materials to be resistant against chemical and biological corrosion. Recent studies on corrosion of Zircaloy-clad SNF indicate growth of oxide films for a time span of a million years to be about 7.6E-03 millimeter (0.3 mil). Given the extremely slow corrosion rate, breach of the relatively thick 22-mil cladding during the time period of interest would probably occur only as a result of mechanical damage or defect. Therefore, to account for cladding defects and mechanical damage, two alternative assumptions were made regarding the fraction of the SNF that is exposed to water. In a few cases, it was assumed that 1% of the SNF is exposed to water immediately after the WP is breached and that the cladding protects the remaining SNF from exposure to water for the duration of the run. In most cases, it was assumed that all of the SNF is immediately exposed to water upon breach of the WP. The basis of these assumptions is that it conservatively accounts for defects and

mechanical damage during storage, shipping, or packing, and that it provides a basis for examining the sensitivity of the results to assumptions about cladding integrity.

3.21 The mass of aluminum (Al) filler material that may be used to fill the otherwise empty spaces in the SNF canister is calculated based on the assumption that the filler will be Al shot with a bulk density of 75% of 2.7 g/cm^3, which is the approximate theoretical density of Al metal and an assortment of Al alloys (Ref. 55, Table 11, p. 7). A high solids fraction approaching 75% is not expected with Al shot (Ref 12, Sec. 3.1.8). The basis of this assumption is the observation that if a solids fraction of 75% is assumed, the calculated mass will exceed the mass that would be experienced in practice and the higher mass will be conservative from a structural perspective. The higher mass is not likely to be conservative from a shielding or criticality perspective.

3.22 It is assumed that the Al shot filler inside the DOE canister will have a composition similar to the average composition of the Al alloys in Table 1 of Reference 15 (p. 373) but with ~1 weight percent Gd (as $GdPO_4$), added as a neutron absorber. The basis of this assumption is that mixing $GdPO_4$ into the alloy appears likely because it would assure an even distribution of Gd throughout the SNF canister.

3.23 It is assumed that the addition of $GdPO_4$ to the Al shot has no effect on the degradation rate of the Al alloy. The basis for this assumption is that no specific information is available to support a different degradation rate.

3.24 It is assumed that the ThO_2 SNF pellets degrade at the same rate as microcrystalline ThO_2 (Ref. 37, Fig. 3 and 4, Equations 2 and 11). The basis of this assumption is that the actual degradation rate of the sintered ceramic ThO_2 SNF pellets should be much lower than the dissolution rate of microcrystalline ThO_2, making the degradation rate conservative with respect to possible losses of Th and U from the SNF.

3.25 It is assumed that the UO_2-ThO_2 binary pellets degrade at the same rate as the ThO_2 pellets. The basis of this assumption is that the UO_2 fraction in the binary pellets is small enough that no significant effect is expected (Ref. 16, Figure 2 and Table 1)

4. USE OF COMPUTER SOFTWARE AND MODELS

This section describes the computer software used to carry out the analysis.

EQ3/6 Software Package–The EQ3/6 software package originated in the mid-1970s at Northwestern University (Ref. 22). Since 1978, Lawrence Livermore National Laboratory (LLNL) has been responsible for maintenance of EQ3/6. The software has most recently been maintained under the sponsorship of the Civilian Radioactive Waste Management Program of the United States Department of Energy (DOE). The major components of the EQ3/6 package include: EQ3NR, a speciation-solubility code; EQ6, a reaction path code which models water/rock interaction or fluid mixing in either a pure reaction progress mode or a time mode; EQPT, a data file preprocessor; EQLIB, a supporting software library; and several (>5) supporting thermodynamic data files. The software deals with the concepts of thermodynamic equilibrium, thermodynamic disequilibrium, and reaction kinetics. The supporting data files contain both standard state and activity coefficient-related data. Most of the data files support the use of the Davies or B-dot equations for the activity coefficients; two others support the use of Pitzer's equations. The temperature range of the thermodynamic data in the data files varies from 25°C only, for some species, to a full range of 0-300°C for others. EQPT takes a formatted data file (a "data0" file) and writes an unformatted near-equivalent called a data1 file, which is actually the form read by EQ3NR and EQ6. EQ3NR is useful for analyzing groundwater chemistry data, calculating solubility limits, and determining whether certain reactions are in states of partial equilibrium or disequilibrium. EQ3NR is also required to initialize an EQ6 calculation.

EQ6 represents the consequences of exposing an aqueous solution to a set of reactants, which react irreversibly. It can also represent fluid mixing and the consequences of changes in temperature. This code operates both in a pure reaction progress frame and in a time frame. In a time frame calculation, the user specifies rate laws for the progress of the irreversible reactions. Otherwise, only relative rates are specified. EQ3NR and EQ6 use a hybrid Newton-Raphson technique to make thermodynamic calculations. This is supported by a set of algorithms that create and optimize starting values. EQ6 uses an ordinary differential equation integration algorithm to solve rate equations in time mode. The codes in the EQ3/6 package are written in FORTRAN 77 and have been developed to run under the UNIX operating system on computers ranging from workstations to supercomputers. Further information on the codes of the EQ3/6 package is provided (Refs. 22, 23, 24, and 25).

Solid-Centered Flow-Through Mode–EQ6 Version 7.2b, as distributed by LLNL, does not contain an SCFT mode. To add this mode, it is necessary to change the EQ6 source code, and recompile the source. However, by using a variant of the "special reactant" type built into EQ6, it is possible to add the functionality of SCFT mode in a very simple and straightforward manner.

The new mode is induced with a "special-special" reactant. The EQ6 input file nomenclature for this new mode is jcode=5; in the Daveler format, it is indicated by the reactant type

DISPLACER. The jcode=5 is immediately trapped and converted to jcode=2, and a flag is set to indicate the existence of the DISPLACER reactant. Apart from the input trapping, the distinction between the DISPLACER and SPECIAL reactants is seen only in one 9-line block of the EQ6 FORTRAN source code (in the reacts subroutine), where the total moles of elements in the rock plus water system (mte array) is adjusted by adding in the DISPLACER reactant, and subtracting out a commensurate amount of the total aqueous elements (mteaq array).

This new EQ6 mode acts as a substitute for the allpost/nxtinput method described in References 19 and 27.

4.1 SOFTWARE

The software package, EQ3/6, Version 7.2b, was approved for QA work by LLNL (Memorandum to File from Royce E. Monks, dated March 28, 1997, QA designator 97/026). An installation and testing report (Ref. 20) was written and submitted to Software Configuration Management (SCM), and the proper installation was verified, before the runs described in this calculation were made. The implementation of the SCFT mode is covered by the Software Change Request (SCR) LSCR198 (Ref. 17), and the Software Qualification Report (SQR) for Media Number 30084-M04-001 (Ref. 18). The SCFT addendum was installed on three of the central processing units (CPUs) identified in block 16 of the SCR, and the installation and test reports were filed and returned to SCM before the calculations were run. All the EQ6 runs were performed on a Sandia National Laboratory system, CPU # R433480, a Dell Optiplex G1 450 MHz Pentium II. In this study, EQ3/6 was used to provide the following:

1) A general overview, of the expected, chemical reactions

2) The degradation products from corrosion of the waste forms and canisters

3) An indication of the minerals, and their amounts, likely to precipitate within the WP.

The programs have been used within the range of parameters for which they have been verified and are appropriate for the application. The calculation inputs include several EQ6 database files with the file extensions "nuc" or "ymp" and other EQ6 input files specific to different WP degradation scenarios with the extension "6i". There are several types of EQ6 output files and they are not all important for the purpose of this calculation. The EQ6 input and output files pertinent for this calculation are described further in Section 5 and can be found on the compact discs (CDs) in Attachment II.

The EQ3/6 package has been verified by its present custodian, LLNL. The source codes were obtained from SCM in accordance with the Administrative Procedure AP-SI.1Q, *Software Management* (Ref. 48). The code was installed on the Pentium PCs according to an M&O-approved Installation and Test procedure (Ref. 20).

4.2 SOFTWARE ROUTINES

Spreadsheet analyses were performed with Microsoft Excel Version 97, installed on a PC. The specific spreadsheets used for results reported in this document, are included in the attached CDs (Attachment II).

The volume and area of some of the WP components inside of the DOE SNF Canister were calculated using the software routine eqsetup.exe, version 1 provided in the attached CDs (Attachment II). A listing of the code and instructions for running the program is provided in the file eqsetup.c also provided in Attachment II. A change history is not provided because this is the first version of the routine, which was also used and described in Reference 21 (Section 4.2 and Attachment II). The program was written in ANSI C and compiled under Microsoft C++, Version 6.0. Besides calculating volumes and areas, the program computes moles of all materials described in the input file "data.in." Besides "data.in," three files are necessary to run the routine: "template.in," "ratefacs.in," and "atwts.in." The output file "junk.out" provides the volume, area, and mole calculation results. The accuracy of the volume and area calculations were checked in spreadsheet "doecan_EDA2.xls", sheet "densities and moles react"(Attachment II). Also included in the attached CDs is the output file "LWBRjunk.txt" that contains the "junk.out" results from eqsetup.

Some of the calculation results were extracted into text files using the program PP, which is included in the attached CDs (Attachment II). PP is a plotting routine, but it is also possible to extract the data from a plot in PP into a text file that can be imported into another program, such as Microsoft Excel. PP is exempt from the requirements of procedure AP-SI.1Q (Ref. 48). Section 2.1.5 of the procedure states: "Software used solely for visual display or graphical representation of data which is used in a product which is checked and approved in accordance with applicable procedures and meets stated acceptance criteria is exempt."

4.3 MODELS

None used.

5. CALCULATION

The existing database supplied with the EQ3/6 computer package is sufficiently accurate for the purposes of this calculation. The data have been carefully scrutinized by many experts over the course of several decades and carefully selected by LLNL (LLNL) for incorporation into the data base (Refs. 22, 23 ,24 and 25). These databases are periodically updated and/or new databases added, such as one including extensive data on the lanthanides (Ref.26). Every run of either EQ3 or EQ6 documents automatically which database is used. The databases include references internally for the sources of the data. The reader is referred to this documentation, included in the electronic files labeled data0 that accompany this calculation, for details (Attachment II). Nevertheless, the quality of data needs to be verified in the future.

The calculations begin with selection of data for compositions, amounts, surface areas, and reaction rates of the various components of Shippingport LWBR SNF WPs. These quantities are recalculated to the form required for entry into EQ6. For example, weight percentages of elements or component oxides are converted to mole fractions of elements; degradation rates in micrometers/year are converted into moles per square centimeter per second, etc. Spreadsheets (Attachment II) and Reference 12 provide details of these calculations, and the general procedure is also described in detail in Reference 27 (Section 4). The final part of the input to EQ6 consists of the composition of J-13 well water together with a rate of influx to the WP that corresponds to suitably chosen percolation rates into a drift and drip rate into a WP (Section 5.1.1.3). The EQ6 output provides the results representing the chemical degradation of the WP, or components thereof. Sometimes the degradation of the WP is divided into stages, e.g., degradation of HLW glass before breach and exposure of the SNF assemblies and basket materials to the water. The results include the compositions and amounts of solid products and of substances in solution. Details of the results are presented below.

5.1 CALCULATION INPUTS

5.1.1 WP Materials and Performance Parameters

This section provides a brief overview of the physical and chemical characteristics of Shippingport LWBR SNF WPs, and describes how the WP is represented in the EQ6 inputs. The conversion of the WP physical description, into parameters suitable for the EQ6 input files, is performed by the spreadsheet "doecan_EDA2.xls". Additional details of the description may be found in References 1 and 12 and the references cited therein.

Material nomenclature for the stainless steels and carbon steels used throughout this document includes: SA-240 S31603 stainless steel (hereafter referred to as 316L stainless steel); Unified Numbering System (UNS) N06625 and SA-240 S30403 stainless steel (hereafter referred to as 304L); SA-516 and SA-36 carbon steel (hereafter referred to as A516); and AM350 stainless steel.

5.1.1.1 Physical and Chemical Form of Shippingport LWBR SNF WP

It is convenient to consider the Shippingport LWBR SNF WP as several structural components, specifically:

1) The outer shell, consisting of CRM (Alloy 22)

2) The inner shell composed of 316L stainless steel

3) The "outer web", a carbon steel (A516) structure designed to hold the HLW glass-pour canisters (GPCs) in place

4) The GPCs, the 304L containers of the solidified HLW glass

5) The DOE SNF canister (sometimes called the "18 inch canister") composed of 316L stainless steel

6) The SNF assembly, exclusive of the SNF, a basket constructed of 316 L stainless steel plates and a spacer, AM350 stainless steel grids which held the seed assembly in place, and A516 carbon steel impact plates, all of which are inside the DOE SNF canister

7) The Shippingport LWBR (Th/U Oxide) SNF seed assembly

8) Aluminum shot, doped with 3 weight percent $GdPO_4$ neutron absorber, used as filler inside the DOE SNF canister.

The details of each of the above numbered components are in the spreadsheets: "doecan_EDA2.xls" in sheets "SNF Can-long" and "Vol & Area"; "ShipLWBR.xls" in sheets "Al Fill," "Al Shot & AM350" and "Fuel & Glass"; "LWBRshapes.xls" in sheets "seed pellets," "seed lowfuel," "seed highfuel," "assemblies," and "grids" (Attachment II); as well as in Reference 1 (Section 3, pp. 16-23, Tables 3-5 through 3-12, Figures 3-9 and 3-11) and Reference 12.

Table 1 provides a summary of the compositions of the principal steel alloys used in the calculations. Table 2 provides average and maximum degradation rates for the steels. For a comparable specific surface area, the carbon steel (A516) is expected to degrade much more rapidly than the stainless steels (316L, 304L, and AM350). In addition, the stainless steels contain significant amounts of Cr and/or Mo and, under the assumption of complete oxidation (Assumption 3.7), should produce more acid, per volume, than the carbon steel. In Table 1 and all tables from this document, the number of digits reported does not necessarily reflect the accuracy or precision of the calculation. In most tables, three to four digits after the decimal place have been retained, to prevent round-off errors in subsequent calculations.

Table 1. Steel Compositions

Element	A516 Carbon Steel[a]		AM-350 Stainless Steel[b]		304L Stainless Steel[c]		316L Stainless Steel[d]	
	Weight %	Atom Fraction	Weight %	Atom Fraction	Weight %	Atom Fraction	Weight %	Atom Fraction
C	0.30	0.0138	0.09	0.0041	0.03	0.0014	0.03	0.0014
Mn	1.03	0.0103	0.88	0.0088	2.00	0.0199	2.00	0.0202
P	0.04	0.0006	0.04	0.0007	0.05	0.0008	0.05	0.0008
S	0.04	0.0006	0.03	0.0005	0.03	0.0005	0.03	0.0005
Si	0.28	0.0054	0.50	0.0098	0.75	0.0146	0.75	0.0148
Cr			16.50	0.1755	19.00	0.1997	17.00	0.1810
Ni			4.50	0.0424	10.00	0.0931	12.00	0.1132
Mo			2.88	0.0166			2.50	0.0144
N			0.10	0.0039	0.10	0.0039	0.10	0.0040
Fe	98.33	0.9694	74.49	0.7376	68.05	0.6660	65.55	0.6498
Total	100.00	1.0000	100.00	1.0000	100.00	1.0000	100.00	1.0000

Sources: [a] Reference 54 (p. 321, Table 1)
[b] Reference 13 (p. 359)
[c] Reference 57 (p. 2, Table 1)
[d] Reference 56 (p. 2, Table 1)

Table 2. Steel Degradation Rates and Rate Constants

	A516 Carbon Steel	AM-350 Stainless Steel	304L Stainless Steel	316L Stainless Steel
Molecular Weight (g/mol)	100.00[a]	100.00	100.00	100.00
Density (g/cm^3)	7.85[b]	7.90[c]	7.94[d]	7.98[d]
Low Rate (μm/year)	35[e]	0.1[f]	0.1[f]	0.1[f]
Low Rate Constant[g] (mol/cm^2·s)	8.706E-12	2.503E-14	2.516E-14	2.529E-14
Moderate Rate (μm/year)	100[e]	1[f]	1[f]	1[f]
Moderate Rate Constant (mol/cm^2·s)	2.488E-11	2.503E-13	2.516E-13	2.529E-13
Average Rate (μm/year)	72.271364[h]	1.9996307[i]	34.405015[i]	1.9996307[i]
Average Rate Constant (mol/cm^2·s)	1.79776E-11	5.00579E-13	8.65642E-12	5.05648E-13
High Rate (μm/year)	131.12667[h]	33.274895[i]	207.53885[i]	33.274895[i]
High Rate Constant (mol/cm^2·s)	3.2618E-11	8.32990E-12	5.22175E-11	8.41425E-12

NOTES: [a]The molecular weight of all WP components was set to 100 g to simplify inputs to EQ6.
[g]This rate constant (and all the rate constants in the following tables) must be multiplied by the normalized surface area (sk in the EQ6 input file) in cm^2 of each WP component to calculate the actual degradation rate in 100-g moles/s of that component.

Sources: [b] Reference 40 (p. 21)
[c] Reference 13 (p. 360) and Reference 12 (Section 3.3.2)
[d] Reference 55 (p. 7, Table XI)
[e] Reference 28, Figures 5.4-3, 5.4-4, and 5.4-5.
[f] Reference 49 (pp. 11-13)
[h] Values from Reference 29 (p. 2.2-78) were used to derive these rates in spreadsheet "A516_Rate.xls", sheets "Prob" and "Prob_Chart" (Attachment II)
[i] Rates were calculated in spreadsheet "ShipLWBR.xls", "Rates" sheet (Attachment II) using Eq. 3-14 (derived from Fig. 3-15 in Reference 30, Sec. 3.1.5.4.1)

Table 3 gives the molar composition of the HLW glass used in the calculations (Ref. 31). The composition in Reference 31 was simplified to produce the values of weight percent listed in Table 3 (Cells S19-S43, sheet "Composition", spreadsheet "HLW_glass.xls", Attachment II). Minor elements or elements with questionable thermodynamic data were removed (Ag, Cr, Cs, Cu, Li, Mn, Ni, Pb, Th, Ti, Zn), and shorter half-life Pu isotopes were "predecayed" to longer half-life U isotopes: ^{242}Pu was converted to ^{238}U; ^{241}Pu was converted to ^{237}Np, which was converted to ^{233}U; ^{240}Pu was converted to ^{236}U; ^{239}Pu was converted to ^{235}U; and ^{238}Pu was converted to ^{234}U. Since small amounts of neutron absorbers (Ag, Th, Zn) were removed in the simplified glass composition, this approach is conservative for internal criticality analyses. The numbers used in the column "Moles, Norm" are used by EQ6 and represent the moles of each element in 100 grams of glass. This simplification of the HLW glass composition allows the material to be entered as a pseudo-mineral, GlassSRL, in the EQ6 database in "data0.nuc" (Attachment II). If the HLW glass is entered in the database as a mineral, a pH dependent glass degradation rate using the EQ6 transition state theory (TST) formalism (Ref. 25, Section 3.3.3) can be applied.

As was shown in Sections 5.3.2 and 5.3.3 of Reference 32, EQ6 estimates of U loss, from the WP, are not greatly affected by substantial variations in the composition of the HLW glass. For three EQ6 runs (Cases 15, 16, and 17 in Table 10) the effect of having SNF as the only source of U in the WP was examined. For these cases, an additional database entry, GlassNp, having the same composition as Glass SRL but with the U replaced by Np, was used as the EQ6 HLW glass reactant.

The actual HLW glass composition used in the GPCs may vary significantly from these values, since the sources of the HLW glass and melting processes are not currently fixed. For example, compositions proposed for Savannah River Site HLW glass vary by a factor of ~6 in U_3O_8 content, from 0.53 to 3.16 weight percent (Ref. 33, p. 3.3-15, Table 3.3.8.). The Si and alkali metal contents (Na, Li, and K) of the HLW glass have perhaps the most significant bearing on EQ6 calculations. The amount of Si in the HLW glass strongly controls the amount of clay that forms in the WP, and the Si activity controls the presence of insoluble uranium phases such as soddyite $[(UO_2)_2SiO_4 \cdot 2H_2O]$. As the HLW glass degrades in an EQ6 run, the alkali metal content of the corrosion products increases and the pH rises. The Si and alkali metal contents in Table 3 are typical for proposed DOE HLW glasses (Ref. 31).

A pH-dependent rate for HLW glass degradation was derived from Reference 34 (Section 6.3.3.2, Figure 6-31), and normalized in spreadsheet "Glass_rates_110999.xls", sheet "Glass Rates" (Attachment II). The first rate mechanism (described with k_1) in Table 3 is dominant at pH values above 7, while the second rate mechanism (described with k_2) is dominant at pH values below 7. The high glass degradation rate constants in Table 3 are those predicted at 50°C, while the moderate rate constants are those derived for degradation at 25°C (Ref. 34, Section 6.3.3.2, Figure 6-31).

For EQ6 cases 22 through 25 (Table 10) run for this calculation, a different set of pH dependent glass degradation rate constants, a slightly different glass composition (Cells AF19-AF43, sheet

"Composition", spreadsheet "HLW_glass.xls", Attachment II) and a different EQ6 database ("data0.ymp" in Attachment II) were used. These rate constants were derived from Equations 7 and 8 in Reference 35 (Sec. 6.2.3.3) and normalized in the spreadsheet "HLW_glass.xls", sheet "Rates" (Attachment II). The third rate mechanism (described with k_3) in Table 3 is dominant at pH values above 7, while the fourth rate mechanism (described with k_4) is dominant at pH values below 7. The high glass degradation rate constants in Table 3 are those derived for 50°C, while the moderate rate constants are those derived for degradation at 25°C. These glass degradation rates were also used to apply the EQ6 TST rate formalism.

Table 3. HLW Glass Composition[a], Density[b], and Degradation Rates[c]

Element	Moles per 100 g of HLW Glass	
O	2.7666E+00	
U	7.9811E-03	
Ba	1.1211E-03	
Al	8.8317E-02	
S	4.0512E-03	
Ca	1.6572E-02	
P	4.5548E-04	
Si	7.9455E-01	
B	2.9802E-01	
F	1.6824E-03	
Fe	1.7623E-01	
K	7.6706E-02	
Mg	3.4052E-02	
Na	5.9006E-01	
Total	4.8977E+00	
Density(g/cm^3)	2.85	
Total VA Rate Constant[d] = $k_1[H^+]^{-0.4721} + k_2[H^+]^{0.6381}$ (mol/cm^2·s)		
Moderate Rate Constant (k_1)	(liter/cm^2·s)	1.98373E-19
High Rate Constant (k_1)	(liter/cm^2·s)	2.92353E-18
Moderate Rate Constant (k_2)	(liter/cm^2·s)	6.14458E-12
High Rate Constant (k_2)	(liter/cm^2·s)	3.67106E-11
Total Ebert Rate Constant[e] = $k_3[H+]^{-0.4} + k_4[H+]^{0.6}$ (mol/cm^2·s)		
Moderate Rate Constant (k_3)	(liter/cm^2·s)	8.85753E-19
High Rate Constant (k_3)	(liter/cm^2·s)	1.07560E-17
Moderate Rate Constant (k_4)	(liter/cm^2·s)	7.97555E-13
High Rate Constant (k_4)	(liter/cm^2·s)	4.87424E-12

Sources: [a]Reference 31; Attachment II ("HLW_glass.xls", sheet "Composition")
[b]Reference 58 (p. 26 Fig. 2 and pp 54-57)
[d]Reference 34 (Section 6.3.3.2, Figure 6-31); Attachment II ("Glass_rates_110999.xls", sheet "Glass Rates")
[e]Reference 35; (Section 6.2.3.3, Equations 7 and 8); Attachment II ("HLW_glass.xls", sheet "Rates")

NOTE: [c] In degradation rates, one mole = 100g HLW glass (see note Table 2).

Table 4 summarizes the assumed characteristics of the Shippingport LWBR SNF. No fission product inventory was available, so the calculations used the composition of fresh (unirradiated) SNF. Use of fresh SNF is conservative, since most fission products have significant neutron absorption cross sections, and the unirradiated fuel has a higher fissile content than partially spent fuel. The three types of Shippingport LWBR SNF were also added to the EQ6 thermodynamic database ("data0.nuc" in Attachment II) as the pseudo-minerals FuelBinHi, FuelBinLo, and Th_Fuel, each with a molecular weight of 100g and a large enough solubility product constant to ensure dissolution but prevent precipitation in the WP. This enabled the application of EQ6 TST kinetic rate laws (Ref. 25, Sec. 3.3.3.) to describe the fuel degradation rate. The pH and carbonate dependent fuel degradation rate constants in Table 4 were derived from Reference 37 (Figures 3 and 4, Equations 2 and 11) and normalized in spreadsheet "ShipLWBR.xls", sheet "Fuel Rates" (Attachment II). For Cases 24 and 25 (Table 10), a temperature dependent fuel degradation rate constant was used (Th/U oxide ceramic release rate for 25°C; Ref. 36, Sec. 6.3.6, Table 1) and normalized in spreadsheet "ShipLWBR.xls", sheet "Fuel Rates." When this rate was used, the 3 fuel types were entered in the EQ6 input files as "special reactants" (not minerals entered in the EQ6 database), and a different EQ6 database ("data0.ymp" in Attachment II) was used.

Table 4. Shippingport LWBR (Th/U Oxide) SNF Elemental Composition[a] and Degradation Rates

Element	High Fissile U Binary Fuel (Mole Fraction)	Low Fissile U Binary Fuel (Mole Fraction)	Thoria Fuel (Mole Fraction)
U-233	1.963E-02	1.637E-02	
U-234	2.567E-04	2.140E-04	
U-235	1.783E-05	1.487E-05	
U-236	3.947E-06	3.290E-06	
U-238	7.240E-05	6.035E-05	
Th	3.134E-01	3.167E-01	3.333E-01
O	6.667E-01	6.667E-01	6.667E-01
Sum	1.000E+00	1.000E+00	1.000E+00
Molecular Weight[d]	100	100	100
Density (g/cm^3)[a,e]	9.70155	9.63832	9.67752
Total SNF Rate Constant[b] = $k_1[H^+]^{0.93} + k_2[CO_3^{2-}]^{0.88}$ (mol/cm^2·s)			
		k_1	k_2
Low Rate Constant (liter/cm^2·s)		9.27603e-14	2.72497E-14
Average Rate Constant (liter/cm^2·s)		9.27603e-13	2.72497E-13
High Rate Constant (liter/cm^2·s)		9.27603e-12	2.72497E-12
Special 25°C Rate Constant[c] (mol/cm^2·s)			4.20033E-16

Sources: [a]Reference 1, Tables 3-1 and 3-5; Attachment II ("LWBRshapes.xls", sheets "seed lowfuel" and "seed highfuel"; "ShipLWBR.xls", sheet "Fuel & Glass")
[b] Reference 37, Figures 3 and 4, Equations 2 and 11; Attachment II ("ShipLWBR.xls", sheet "Fuel Rates")
[c]Reference 36, Section 6.3.6, Table 1; Attachment II ("ShipLWBR.xls", sheet "Fuel Rates")

NOTES: [d]One mole = 100g fuel (see note Table 2)
[e]Each fuel density used in this calculation was determined using the following formula (Attachment II, "LWBRshapes.xls", sheets "seed lowfuel" and "seed highfuel"), and data from Reference 1, Table 3-5: density = theoretical density × percent theoretical density × (1- void fraction).

The outer web is composed of A516 carbon steel, and serves two purposes: it centers and holds in place the DOE SNF canister; and it separates the GPCs and prevents them from transmitting undue stress to the SNF canister in the event of a fall (tip-over) of the entire WP. At the center of the outer web is a thick (3.175 cm) cylindrical support tube, also constructed of A516. In a breach scenario, the outer web will be exposed to water and corrosion before the rest of the WP, and is expected to degrade within a few hundred to a few thousand years. The oxidation of iron in the outer web steel into hematite (Fe_2O_3) can decrease the void space in the WP by ~13%, while iron transformation to goethite (FeOOH) can decrease the void space by ~22% (Ref. 2) since goethite has a larger molar volume than hematite (Table 9). Thus the void space can be significantly reduced, soon after breach of the WP, by the alteration of the outer web.

The DOE SNF canister fits inside the central support tube of the outer web. The canister is composed primarily of 316L, with two internal, thick impact plates of carbon steel (approximated as A516 in the calculations). A basket structure constructed of 316L stainless steel plates is located within the DOE SNF canister to maintain the position of the assembly in the center of the canister. For Shippingport LWBR SNF WP degradation scenarios, void space within the DOE SNF canister surrounding the SNF seed assembly was filled with Al shot

containing ~1 weight percent Gd (as $GdPO_4$) (see Assumption 3.22). The composition, density, and degradation rates of the Al alloy used in this calculation are in Table 5.

Table 5. Elemental Composition[a], Degradation Rate Constant[b], and Density[c] of Aluminum Fill Material

Element	Weight %	Mole Fraction
Al	95.34	0.9673
Ti	0.15	0.0008
Cu	0.27	0.0012
Si	0.59	0.0058
Zn	0.25	0.0010
Mg	0.99	0.0111
Mn	0.15	0.0007
Fe	0.69	0.0034
Gd	0.98	0.0001
P	0.19	0.0017
O	0.40	0.0069
Sum	100.00	1.0000
Molecular Weight[d]		100
Density (g/cm^3)		2.025
Degradation Rate Constant (mol/cm^2·s)		2.53587E-13

Sources: [a] Reference 15, Table 1, p. 373 but with added $GdPO_4$; Attachment II ("ShipLWBR.xls", sheet "Al Shot & AM350")
[b] Reference 38, p. 603; Attachment II ("ShipLWBR.xls", sheet "Rates")
[c] Reference 12, Section 3.1.8

NOTE: [d]One mole = 100g Al fill material (see note Table 2)

5.1.1.2 Chemical Composition of J-13 Well Water

It was assumed that the water composition entering the WP would be the same as for water from well J-13 (Assumptions 3.2 and 3.3). This water has been analyzed repeatedly over a span of at least two decades (Ref. 60, DTN: MO0006J13WTRCM; Ref. 6, DTN: LL980711104242.054). The composition of J-13 water as used in this calculation has been adjusted slightly (see assumptions 3.9 and 3.13). Tables 6 and 7 contain the EQ3NR input file constraints for J-13 water composition and the EQ6 input file elemental molal composition for J-13 water used for this calculation.

The "Basis Species" column of Table 6 lists the chemical species names recognized by EQ3NR and EQ6. Since some of the components of J-13 water, as analyzed (Ref. 60, DTN: MO0006J13WTRCM; Ref. 6, DTN: LL980711104242.054), are in a different chemical form than the species listed in this column, these components must be substituted or "switched" with the basis species for input into EQ6 and are listed in the "Basis Switch" column. Basis species listed as "Trace" in the "Basis Switch" column are not found in J-13 water, as analyzed (Ref. 60, DTN: MO0006J13WTRCM; Ref. 6, DTN: LL980711104242.054), but are in the composition

of other WP components and must be input at a minimum concentration for numerical stability in EQ6 calculations.

Table 6. EQ3NR Input File Constraints for J-13 Water Composition

Basis Species	Basis Switch	Concentration	Units
redox		-0.7[e]	log fO_2
Na+		4.580E+01[d]	mg/L
SiO_2(aq)		6.097E+01[d]	mg/L
Ca++		1.300E+01[d]	mg/L
K+		5.040E+00[d]	mg/L
Mg++		2.010E+00[d]	mg/L
Li+		4.800E-02[e]	mg/L
H+		8.1[d]	pH
HCO_3-	CO_2(g)	-3[d]	log fCO_2
O_2(aq)		5.600E+00	mg/L
F-		2.180E+00[d]	mg/L
Cl-		7.140E+00[d]	mg/L
NO_3-	NH_3(aq)	8.780E+00[d]	mg/L
SO_4--		1.840E+01[e]	mg/L
$B(OH)_3$(aq)		7.660E-01[e]	mg/L
Al+++	Diaspore	0	Mineral
Mn++	Pyrolusite	0	Mineral
Fe++	Goethite	0	Mineral
HPO_4--		1.210E-01[e]	mg/L
Ba++	Trace	1.000E-16	Molality[a]
CrO_4--	Trace	1.000E-16	Molality[a]
Cu++	Trace	1.000E-16	Molality[a]
Gd+++	Trace	1.000E-16	Molality[a]
MoO_4--	Trace	1.000E-16	Molality[a]
Ni++	Trace	1.000E-16	Molality[a]
Np++++[b]	Trace	1.000E-16	Molality[a]
Pb++[c]	Trace	1.000E-16	Molality[a]
Pu++++[c]	Trace	1.000E-16	Molality[a]
Th++++	Trace	1.000E-16	Molality[a]
$Ti(OH)_4$(aq)	Trace	1.000E-16	Molality[a]
UO_2++	Trace	1.000E-16	Molality[a]
Zn++	Trace	1.000E-16	Molality[a]

DTN: MO0006J13WTRCM.000, LL980711104242.054

NOTES: [a] A trace concentration (1.0E-16 molal) is added for elements that are not in J-13 water as analyzed, but are in the composition of the WP components, to ensure numerical stability in EQ3/6 runs.
[b] Only included for Cases 9, 15, 16, 17 and 25 in Table 10.
[c] Only included for Case 9.

Sources: [d] Ref. 60 (DTN: MO0006J13WTRCM.000).
[e] Ref. 6 (DTN: LL980711104242.054).

Table 7. EQ6 Input File Elemental Molal Composition for J-13 Water

Element	Mole/kg	Element	Mole/kg
O	5.55E+01	Mg	8.27E-05[a]
Al	2.55E-08[b]	Mn	3.05E-16[b]
B	1.24E-05[b]	Mo	1.00E-16
Ba	1.00E-16	N	1.42E-04[a]
Ca	3.24E-04[a]	Na	1.99E-03[a]
Cl	2.01E-04[a]	Ni	1.00E-16
Cr	1.00E-16	S	1.92E-04[a]
Cu	1.00E-16	Si	1.02E-03[a]
F	1.15E-04[a]	Th	1.00E-16
Fe	3.60E-12[b]	Ti	1.00E-16
Gd	1.00E-16	U	1.00E-16
H	1.11E+02[b]	Zn	1.00E-16
C	2.09E-03[a]	K	1.29E-04[a]
P	1.26E-06[b]	Li	6.92E-06[b]
Np	1.00E-16	Pb	1.00E-16
Pu	1.00E-16		

DTN: MO0006J13WTRCM.000, LL980711104242.054

Sources: [a] Ref. 60 (DTN: MO0006J13WTRCM.000).
[b] Ref. 6 (DTN: LL980711104242.054).

5.1.1.3 Drip Rate of J-13 Well Water into a WP

It is assumed (Assumption 3.13) that the drip rate onto a WP is the same as the rate at which water flows through the WP. The drip rate is taken from a correlation between percolation rate and drip rate (Ref. 39, Tables 2.-55 and 2-56). Specifically, percolation rates of 40 mm/year and 8 mm/year correlate with drip rates onto the WP of 0.15 m^3/year and 0.015 m^3/year, respectively. The choice of these particular percolation and drip rates is discussed in detail in Reference 27 (Section 5.1.1.3, p. 19).

For the present study, the range of allowed drip rates was extended to include an upper value of 0.5 m^3/year and a lower value of 0.0015 m^3/year. The upper value corresponds to the 95 percentile upper limit for a percolation rate of 40 mm/year, and the lower value is simply $1/10^{th}$ the mean value for the percolation rate of 8 mm/year (Ref. 39, Figure 2-114).

5.1.1.4 Calculation of Evaporated Salts Composition

The purpose of this calculation was to provide an estimate of the solids that might precipitate within the Shippingport LWBR SNF assembly. The concern was that the precipitated salts would displace either air or water, substantially changing the neutron moderating properties of the WP. The composition of J-13 water, as used for the Shippingport LWBR EQ6 runs, was numerically "evaporated," precipitating minerals in a sequence that assured charge balance. The

results are given in Table 8. The details of the calculation are given in spreadsheet "LWBRj13evaporIIK3.xls" included with the attached CDs (Attachment II).

Table 8. Concentrations[a] and Densities[b] of Salts from Evaporated J-13 Well Water

Mineral	Concentration (moles/liter)	Concentration (g/liter)	Density (g/cm^3)
AlO(OH)	2.553E-08	1.531E-06	3.40
$Ca_2B_6O_{11}:5H_2O$	2.065E-06	8.488E-04	2.42[c]
$CaCO_3$	1.287E-04	1.288E-02	2.71
KF	1.147E-04	6.666E-03	2.48
KCl	1.416E-05	1.056E-03	1.98
Li_2O	3.458E-06	1.033E-04	2.01
$MgCO_3$	8.270E-05	6.973E-03	2.96
NaCl	1.872E-04	1.094E-02	2.17
$Na_2CO_3:H_2O$	9.025E-04	1.119E-01	2.25
$CaSO_4$	1.915E-04	2.608E-02	2.96
SiO_2	1.015E-03	6.097E-02	2.32

Sources: [a]Attachment II, spreadsheet "LWBRj13evaporIIK3.xls"
[b]Reference 59, pp. B-65, B-67, B-92, B-93, B-110, B-111, B-121, B-125, and B-181.
[c]Attachment II, "Data0.nuc" (Calculated from the molecular weight and molar volume of Colemanite)

5.1.1.5 Densities and Molecular Weights of Solids

For input to criticality calculations, one must convert moles of solids to volume of solids. A few solid phases contribute the overwhelming bulk of the total volume; Table 9 provides some of the densities and molar volumes for these phases. The current version of EQ6 (Section 4) performs the volume calculations for each element automatically.

Table 9. Densities and Molecular Weights of Precipitated Solids

Solid	Density (kg/m^3)	Molecular Weight (g/mole)[c]	Molar Volume (cm^3/mol)[c]	Calculated Density (g/cm^3)
Boehmite (AlOOH)	3030[b]	59.988	19.535	3.071
Hematite (Fe_2O_3)	5240[b]	159.692	30.274	5.275
Pyrolusite (MnO_2)	5060[a]	86.937	17.181	5.060[a]
Goethite (FeOOH)		88.854	20.820	4.268
Ni_2SiO_4		209.463	42.610	4.916
Trevorite ($NiFe_2O_4$)		234.382	44.524	
Nontronite-Ca		424.293	131.100	3.236
Nontronite-K		430.583	135.270	3.183
Nontronite-Mg		421.691	129.760	3.250
Nontronite-Na		425.267	132.110	3.219

Sources: [a] Reference 42, p. 500.
[b] Reference 10, p. B-121.
[c] Attachment II (EQ3/6 Data base, "data0.nuc"), g/mol, except for pyrolusite, which is calculated from the density and molecular weight. Trevorite given same molar volume as magnetite in EQ6 database.

5.1.1.6 Atomic Weights

Atomic weights were taken from References 43 and 44 (Chart of the Nuclides), and are listed in Attachment II (spreadsheet "ShipLWBR.xls", sheet "Atomic Weights").

5.2 DATA CONVERSION

The data presented in Section 5.1 are not in a form suitable for entry into EQ3/6. The transformation to EQ3/6 format involves converting mass fractions to mole fractions; normalizing surface areas, volumes, and moles to 1 liter reactive water in the system; and converting rates to $mol/cm^2 \cdot s$. Most of these conversions are straightforward and are performed in the spreadsheets that are included in the attached CDs for this document (Attachment II). Reference 27 (Section 4) describes the conversion process in detail.

5.3 EQ6 CALCULATIONS AND SCENARIOS REPRESENTED

The rationale for selection of scenarios in EQ6 simulations is to provide conservative assessments of solubility and transport of fissile materials (i.e., U or Th compounds) and neutron absorber species (i.e., Gd) in the WP. An internal criticality is possible if the fissile material remains behind in the WP and the Gd and other neutron absorbers are flushed from the system. Soluble U carbonate complexes will form in the high pH solutions produced when the HLW glass degrades. The proposed criticality control material, an Al alloy doped with $GdPO_4$, will release Gd into the WP solution at the degradation rate of the alloy (Table 5). Since there will be a simultaneous release of phosphate (from the HLW glass and WP steel components as well as from the Al fill material) into the WP solution, precipitation of $GdPO_4$ will be likely. Gadolinium phosphate will hydrate slightly when exposed to water, to form $GdPO_4 \cdot H_2O$. The latter is very sparingly soluble in neutral solutions (Ref. 8), though its solubility does increase at low and high pH; complexation at high pH is particularly enhanced by dissolved carbonate (Ref. 45). Conditions of low pH could be achieved when steel degrades separately from the HLW glass. The effects of pH, fugacity of $CO_2(g)$, and phosphate concentration on Gd solubility are discussed in detail in Reference 2 (Section 5.3.1). Figure 1 predicts how concentration of the major soluble forms of Gd varies with pH for the $CO_2(g)$ fugacity of 10^{-3} used in the present calculation, assuming that the only source of Gd and phosphate is $GdPO_4 \cdot H_2O$ from the Al fill material (Ref. 2, Fig. 5-1; Attachment II, spreadsheet "LWBR_gd_conc_needed_for_loss.xls"). The dashed lines indicate Gd solubilities necessary to achieve 10% Gd loss from the Shippingport LWBR WP in one million years at the specified J-13 water drip rates (Attachment II, spreadsheet "LWBR_gd_conc_needed_for_loss.xls").

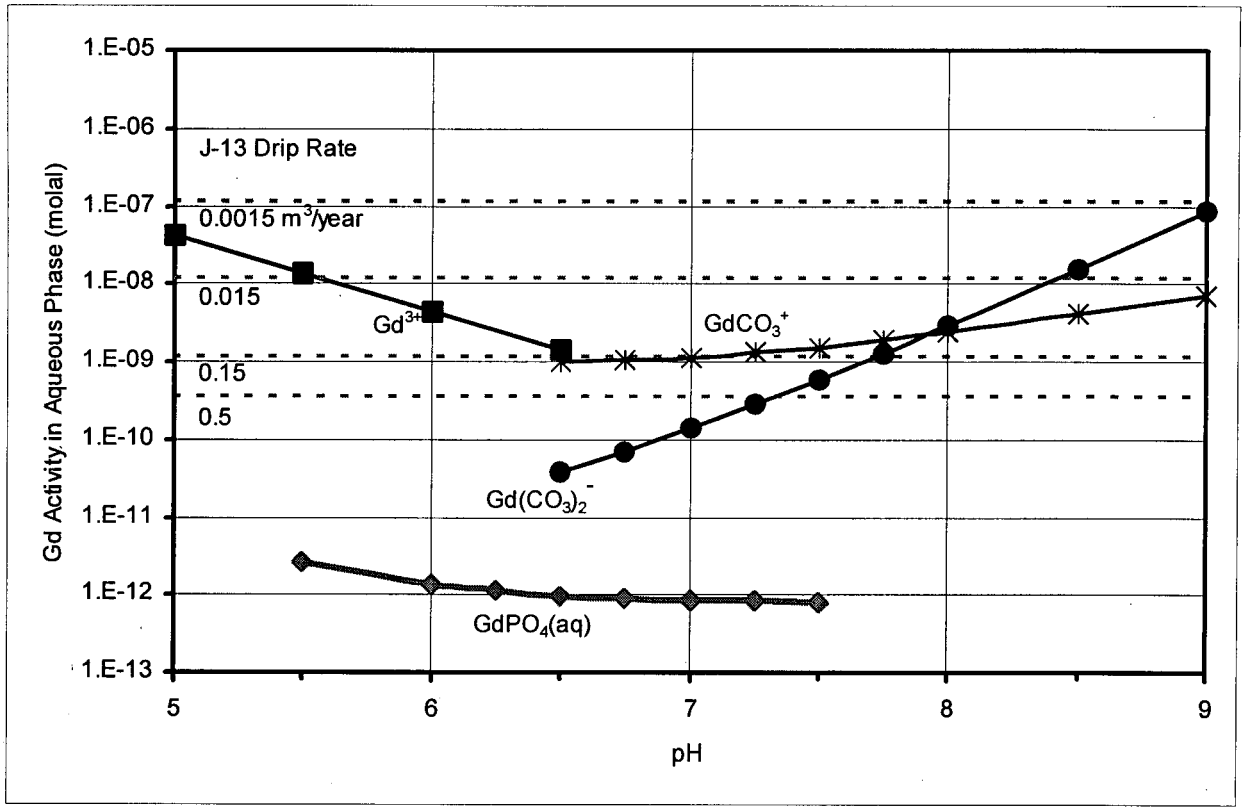

NOTE: The unbroken lines represent the approximate solubility of $GdPO_4 \cdot H_2O$, in terms of major species. The dashed lines represent the solubilities necessary to achieve 10% Gd loss in one million years at the specified drip rates.

Figure 1. Concentration of Major Soluble Forms of Gd as a Function of pH

For these conditions, significant Gd loss would not be expected at a drip rate of 0.0015 m^3/year and might occur at a drip rate of 0.015 m^3/year only if pH values were less than 5.5 or greater than 8.5 for a million years. Gadolinium losses would be possible over the entire pH range shown in Figure 5-1 for the two highest drip rates used in this calculation, except at pH values between 6.5 and 7.0. for a drip rate of 0.15 m^3/year. At the two highest J-13 drip rates, significant Gd losses would be most probable when pH values are less than 6 and greater than 8 for one million years. As mentioned above, steel degradation tends to lower pH while degradation of HLW glass can produce high pH conditions. At very high J-13 water drip rates, the duration of these pH changes is decreased, so that near neutral (~7) pH values are more dominant over long time periods. The EQ6 run conditions used for this calculation (Section 5.3.1) were chosen to emphasize conditions that could create either acid or alkaline conditions, and to determine if these are of sufficient duration to induce Gd loss.

The "*Disposal Criticality Analysis Methodology Topical Report*" document defines the internal and external degradation scenarios for disposal criticality analysis (Ref. 46, pp. 3-7 through 3-11). The internal degradation configurations are based on the assumption that groundwater drips

onto the upper surface of the WP and penetrates it. Groundwater accumulates inside the WP, which could dissolve and flush either neutron absorber or the SNF from the WP. Following is a summary of three groups of degradation configurations from Reference 46:

1. WP internals degrade faster than the waste forms
2. WP internals degrade at the same rate as the waste form
3. WP internals degrade slower than the waste forms.

The WP internals include all components within the WP, including neutron absorber materials except SNF. The waste forms refer to SNF. The above configurations set the framework in which EQ6 scenarios could be developed. The scenarios are based on sequence of chemical reactions as a function of time and can be divided into two general categories: single-stage cases and two multiple-stage cases.

Single-Stage Cases–In these calculations, all WP internals, including SNF, come in contact with groundwater simultaneously. These cases correspond to an extreme in which the zirconium cladding is breached immediately, thereby exposing all or a portion of the spent fuel as soon as the WP corrosion barriers are breached. These cases result in the highest dissolved radionuclide levels, and might provide the most conservative estimate of fissile material and neutron absorber loss.

Multiple-Stage Cases–These EQ6 calculations start with the breach of the WP allowing groundwater to come in contact with WP internals outside the DOE SNF canister ("stage A"); during this stage the DOE SNF canister remains intact. The second stage ("stage B") starts with the breach of the DOE SNF canister and interaction of groundwater with material inside DOE SNF canisters, as well as waste forms and unaltered reactants remaining from stage A. These cases were designed to produce the lowest possible pH, by first exposing the HLW glass to J-13 well water to remove alkalinity, prior to exposure of the SNF in the second stage.

In total, 25 cases of single and multiple-stage EQ6 simulations with different steel and HLW glass degradation rates, as well as varied water fluxes through the WP, were run. These cases are discussed in the following sections.

5.3.1 EQ6 Run Conditions and Nomenclature

The EQ6 codes were used to run the 25 cases summarized in Table 10. In general, each case could be classified as single or multiple-stage. Cases 1-4, 11-21, and 23-25 are single-stage, and involve simultaneous exposure of the SNF and the WP materials to J-13 water. Considering that the SNF pellets are within zirconium cladding, for a conservative approach, it was assumed (Assumption 3.20) that cladding is fully breached immediately after contact with water.

The "Root File Names" column in Table 10 gives the root file names used to describe the runs. The EQ6 input files corresponding to these runs end with the extension ".6i" (e.g., L01x1231.6i is an EQ6 input file name for Case 3); these input files are included with the attached CDs

accompanying this calculation (Attachment II). Each EQ6 run has associated tab-delimited text files, also included in the attached CDs (e.g., "L01x1231.elem_aqu.txt" for Case 3). The text files list total moles of elements in the aqueous phase ("?.elem_aqu.txt"), total moles of each element precipitated as minerals ("?.elem_min.txt"), and total moles of each element ("?.elem_tot.txt"), which is the sum of moles in the aqueous and mineral phases plus the unreacted, or remaining moles of reactants (WP components). Since the HLW glass and SNF WP components were entered into the "data0.nuc" file as "minerals" for this calculation, the remaining moles of these reactants were not included in the "?.elem_tot.txt" files. Several input files, corresponding to separate EQ6 runs, may be grouped into a "Case". Most of the important run conditions could be inferred from the root file name. Evaluation of root file names for most cases from left to right is as follows:

The first letter "L" corresponds to Shippingport LWBR.

The second and third characters (first and second digits after "L") correspond to revision or continuation of input file for the single-stage runs; for each case, the numbers range from 00 to 99. Single-stage runs that do not converge usually require removal of the exhausted reactants and restart of the run (labeled 0-2). There are some exceptions. Those containing an "&" were done assuming 1% SNF exposure to degradation. Those containing an "@" were done using a U-free HLW glass composition.

The second characters (first digit after "L") in the two-stage runs correspond to revision or continuation of input file, while the third character is "a" for the first stage or "b" for the second stage of the run.

The fourth character corresponds to special run conditions. Hematite and goethite are major iron oxide minerals observed to form in rust, though hematite is thermodynamically more stable, and hematite's stability increases with temperature. Some cases were run with hematite suppressed to assess the effect, if any, this might have on internal and external criticality. These cases have "g" (since goethite is the iron oxide predicted to precipitate) as the fourth character. Other special run conditions and the characters representing them are defined in the note beneath Table 10.

The fifth digit is 1, 2, 3, or 4, corresponding to the low, moderate, average, or high rates of steel corrosion in Table 2.

The sixth digit in this block is 1, 2, 3, 4, or 0, with 1 and 2 corresponding to the moderate and high VA HLW glass corrosion rates listed in Table 3, respectively; 3 and 4 corresponding to the moderate and high Ebert HLW glass corrosion rates listed in Table 3, respectively; and 0 corresponding to no HLW glass present in the EQ6 run.

The seventh digit in the block is 1, 2, 3, 4, or 0, with 1 corresponding to low rates of SNF dissolution, 2 corresponding to average dissolution rates, 3 corresponding to high dissolution rate, 4 corresponding to the 25°C temperature dependent rate (see Table 4), and 0

corresponding to no SNF present in the EQ6 run.

The last digit in the block encodes the choice of J-13 flush rate, with 1, 2, 3 and 4 corresponding to 0.0015 m^3/year, 0.015 m^3/year, 0.15 m^3/year, and 0.5 m^3/year, respectively.

5.3.2 Examination of Cases

Table 10 summarizes all the cases run, as well as total percentage of Gd, U, and Th loss at the end of the EQ6 runs. These losses were calculated in the spreadsheet "LWBRshipGdThU.xls" (Attachment II). The complete output tables (aqueous, mineral, and total moles) for all the cases are included in the attached CDs, as text files (Attachment II). A list of the files included in the attached CDs is given in Attachment I.

Tables 11 through 28 illustrate the limits of system behavior for the two-stage runs. Single-stage runs show Gd, U, and Th loss from the SNF and HLW glass to alteration products and solution as a function of reaction time, and how each output varies depending upon input steel corrosion rates, HLW glass corrosion rates, SNF corrosion rates, and fluid flow rates. The two-stage runs provide information on how the system might behave under a number of extreme scenarios. Examination of the results in Table 10 reveals the following generalizations about Gd, U, and Th release from the WP:

Table 10. Summary of Cases Run, Associated Input File Names, Percent Fuel Exposed to Corrosion, Percent Th, Gd and U Loss[a], and Fe Oxide Corrosion Product

Case	Root File Names[b]	% Fuel Exposed	% Th Loss	Time of Th Loss[c] (years)	% Gd Loss	Time of Gd Loss[c] (years)	% U Loss	Time of U Loss[c] (years)	Fe Oxide
1	l02x1113	100	0.00	316873	2.18	316268	2.46	316873	hematite
2	l01x1211	100	0.29	21964	0.03	207420	94.25	128513	hematite
3	l01x1231	100	0.69	23403	0.03	213220	100.0	23403	hematite
4	l01x2133	100	0.00	316621	1.56	316016	5.11	316621	hematite
5	L0ax2204 L0bx2022	0 100	0.00 0.00	36139 313923	0.00 0.14	36139 301795	13.99 0.19	32527 313923	hematite
6a	L0ax2204 L0b$2022	0 100/10	0.00 0.00	36139 313803	0.00 0.14	36139 301674	13.99 0.18	32527 301674	hematite
6b[d]	L1ax2204 L0b$2022	0 100/10	0.00 0.00	59893 316593	0.00 0.16	59893 310158	2.66 0.16	51750 310158	hematite
7	L1ag2204 L0bg2022	0 100	0.00 0.00	31868 314194	0.00 0.14	31868 314194	17.19 0.28	31143 308130	goethite
8	L0an2204 L0bn2022	0 100	0.00 0.00	36275 311955	0.00 0.32	36275 311955	84.74 0.22	36093 305891	hematite
9	L0ao2204 L0bo2022	0 100	0.00 0.00	4074 311672	0.00 0.06	4074 305608	94.04 0.04	1188 275288	hematite
10	L0Ax1203 L0Bx1021	0 100	0.00 0.00	34938 316237	0.00 0.00	34938 316237	94.15 0.02	10839 310849	hematite
11	L02g1113	100	0.00	316300	2.36	315695	3.44	315695	goethite
12	L02g1211	100	0.26	22607	0.01	159588	94.24	116994	goethite
13	L02g1231	100	0.55	23742	0.01	158018	100.0	94141	goethite
14	L01g2133	100	0.00	306836	2.85	306836	8.71	306836	goethite
15	L1@x1113	100	0.00	316561	2.18	316561	0.09[e]	315956	hematite
16	L1@x1211	100	0.33	23375	0.03	193951	1.93[e]	312475	hematite
17	L0@x1231	100	1.38	20796	0.03	210951	100[e]	20796	hematite
18	L1&x1113	1	0.00	316848	2.18	316244	2.46	316848	hematite
19	L1&x1211	1	0.01	21223	0.03	208537	94.15	21223	hematite
20	L1&x1231	1	0.29	21269	0.03	206896	94.21	21269	hematite
21	L1&x2133	1	0.00	316649	1.56	316044	5.11	316649	hematite
22	L2Ax4404[f] L0B$4022[f]	0 100/10	0.00 0.00	24937 312849	0.00 0.25	24937 300721	94.15 0.00	21117 312849	hematite
23	L02g4333[f]	100	0.00	316282	3.63	316282	84.36	316282	goethite
24	L01x3441[f]	100	0.10	54462	0.04	66678	96.09	314665	hematite
25	L1@x3441[f]	100	0.06	48519	0.05	74080	33.15[e]	315021	hematite

NOTES:
[a] U and Th losses are a percentage of total moles of U and Th in fuel and HLW glass
[b] Explanation of special symbols in root file names:
n = No EDA II liner
@ = U in HLW glass replaced by Np
$ = 100% fuel moles and 10% fuel surface area exposed to corrosion
g = These cases were run with hematite suppressed
x = Hematite not suppressed for these runs
o = Used a different HLW glass composition and degradation rate (Ref. 47, Table 5-3.)
& = Only 1% of fuel moles and surface area exposed to corrosion
[c] Predicted time by which loss occurs
[d] Case 6b was run with the degradation rates in Table 16
[e] U loss is a percentage of total moles of U in the fuel only
[f] These cases used a different EQ6 database ("data0.ymp" in Attachment II)

1. High predicted losses of U (94-95%), mostly from HLW glass degradation, occurred for conditions of low steel degradation rate, high HLW glass degradation rate (VA), and low J-13 water flushing rate. Total predicted loss of U (from both fuel and glass, 6% and 94% of the total moles of U in the WP, respectively) from the WP occurred if a high SNF degradation rate was also used in the run. Under these conditions the HLW glass is completely degraded by ~20,000 years and predicted pH values become very alkaline (9.5 to 10) for a short period of time (from 18,000 to 22,000 years) causing complete SNF degradation by ~25,000 years if a high SNF degradation rate is used. The low J-13 flushing rate prolongs alkaline (pH ~8.5) conditions from HLW glass degradation. High alkalinity increases U solubility through formation of U-carbonate/hydroxide complexes.

2. Low, but significant, predicted U losses (5-17%) occurred for conditions of moderate steel degradation rate, and high J-13 water flushing rate. These conditions would tend to decrease pH (increase acidity) until the WP steel was degraded. Then, the high J-13 flushing rate prevented build up of alkalinity as HLW glass degradation continued, thus decreasing solubility of U and the U concentration in the WP solution compared with the conditions mentioned in number 1.

3. Very low predicted U losses (0-4%) occurred for conditions of low steel, low glass (VA), and low fuel degradation rates, with a high J-13 water flushing rate. Under these conditions, very little SNF degradation occurred while the EDA II liner and HLW glass also persisted to the end of the runs (~317,000 years), buffering pH to values around 8.1. Uranium mobility was controlled largely by formation and stability of soddyite [$(UO_2)_2(SiO_4)\cdot 2H_2O$].

4. Predicted loss of Gd from the WP was low (0-4%). The highest predicted Gd losses (2-4%) occurred for conditions of low HLW glass degradation rate (VA or Ebert), and high J-13 water flushing rate. These conditions would result in early low pH values if steel degradation rates were moderate to high or early neutral to mildly acid WP solutions, if steel degradation rates were low. The low rate of HLW glass degradation and high J-13 flushing rate would tend to buffer the WP solution in the mildly alkaline pH range (~8.1), causing a gradual dissolution of the $GdPO_4 \cdot H_2O$ formed when the Al fill material had degraded. Prolonged, extreme alkaline or acid conditions, required for significant Gd loss (Figure 5-1), were not predicted.

5. Predicted loss of Th from the WP was less than 2% for all the cases run. Highest Th losses occurred for cases in which U losses were high (94-100%). The predicted amount of Th in solution was controlled to very low levels by formation of the extremely insoluble mineral thorianite (ThO_2).

Tables 11 and 12 show selected examples of predicted corrosion product and WP solution compositions for a two-stage EQ6 run, Case 5. For this case, and most of the two-stage runs (Cases 5-9), the run conditions for the first stage are moderate steel and high HLW glass degradation rates (VA) with a J-13 water flushing rate of 0.5 m^3/year. The second stages are run

with moderate steel degradation rates, average fuel degradation rate, and a J-13 flushing rate of 0.015 m^3/year. The dominant elements in the corrosion products besides O and H are Fe, Al, and Si. This reflects the composition of the common mineral phases expected to form during waste package degradation: Fe and Al oxide/hydroxides, and silicate minerals, especially smectites, such as nontronite (Table 9). The general decrease in corrosion product density during WP degradation reflects a decrease in the kg of Fe and an increase in the mass of Si and Al with time.

Table 12 shows how predicted pH and solution elemental composition change in the WP with time. Slightly acid pH is predicted during the first 5000 years of WP degradation, with steel degradation buffering WP chemistry. By 20,000 years, when most WP steels are degraded, the degradation of HLW glass dominates the chemistry as reflected by a pH of 8.45. After degradation of the HLW glass is complete, pH returns to a slightly acid value at the end of the first stage of Case 5 (~36,000 years). During the second stage, the SNF canister, the other steel components inside the canister, and the Al fill material degrade, lowering the pH of the WP solution to 5.5. After these components are degraded, the pH returns to a value close to the pH of the incoming J-13 water, 8.1.

The data in Tables 11 and 12 also show how these pH changes may affect the partitioning of U, Th, and Gd between mineral phases and the WP solution. The predicted mass of U in the corrosion products increases during the first stage when HLW glass is degrading, and then remains nearly constant during the second stage. Table 10 shows that <1% U is lost from the WP during the second stage of Case 5, but that ~14% of WP U (all coming from degradation of HLW glass) is lost by ~32,000 years. This loss probably occurs because U levels in solution are highest just before this time (~20,000 years), during the period of alkaline pH caused by degradation of the HLW glass (Table 12). Predicted losses of Gd during the second stage of Case 5 were less than 1% (Table 10). For the run conditions of this case, EQ6 predicted that all of the Th released from SNF precipitated as thorianite, and most of the Gd released from the Al fill material precipitated as $GdPO_4 \cdot H_2O$.

Table 11. Predicted Elemental Composition of Corrosion Products (kg), Total Mass (kg), and Density in Selected Years for Case 5 (I0Ax2204, I0Bx2022)

Years	99	5332	19989	36145	40827	100030	316900
Element							
O	2.533E+03	4.595E+03	1.020E+04	1.293E+04	1.458E+04	1.634E+04	1.649E+04
Al	5.777E-01	2.332E+01	2.693E+02	3.463E+02	1.103E+03	1.103E+03	1.103E+03
Ba	3.410E-02	1.385E+00	1.698E+01	2.178E+01	2.178E+01	2.173E+01	2.172E+01
Ca	9.560E-01	1.377E+01	1.781E+02	1.456E+02	1.383E+02	1.422E+02	1.522E+02
Cr	0.000E+00	5.242E-01	1.321E-16	8.245E+00	8.244E+00	7.921E-28	0.000E+00
F	8.171E-02	5.633E-01	1.317E+00	1.888E+00	1.764E+00	1.887E+00	1.921E+00
Fe	5.737E+03	9.202E+03	1.272E+04	1.581E+04	1.738E+04	2.107E+04	2.107E+04
Gd	0.000E+00	0.000E+00	0.000E+00	0.000E+00	7.809E+00	7.809E+00	7.798E+00
H	1.357E-01	5.437E+00	5.823E+01	7.546E+01	1.042E+02	1.056E+02	1.075E+02
C	5.847E-12	1.260E-12	5.136E+01	1.690E-11	3.270E-12	1.900E+00	1.900E+00
P	6.920E-01	2.755E+00	6.443E+00	9.236E+00	1.171E+01	1.077E+01	1.093E+01
K	1.003E-01	2.401E+00	6.815E+01	1.195E+01	1.167E+01	1.300E+01	1.479E+01
Mg	1.396E-01	4.231E+00	8.773E+01	5.775E+01	6.370E+01	6.322E+01	6.138E+01
Mn	6.216E+01	1.624E+02	2.391E+02	3.238E+02	3.705E+02	4.836E+02	4.836E+02
Na	6.120E-02	1.479E+00	4.827E+01	1.239E+01	1.004E+01	1.350E+01	1.334E+01
Ni	7.226E-01	2.185E+02	6.794E+02	1.164E+03	1.185E+03	1.187E+03	1.187E+03
S	7.961E-03	0.000E+00	0.000E+00	3.649E-11	0.000E+00	3.085E-15	0.000E+00
Si	2.451E+01	3.560E+02	2.952E+03	3.999E+03	4.029E+03	4.116E+03	4.230E+03
Th	0.000E+00	0.000E+00	0.000E+00	0.000E+00	3.002E-02	4.286E-01	3.075E+00
U	4.400E-01	1.860E+01	1.849E+02	2.357E+02	2.357E+02	2.356E+02	2.352E+02
Total mass	8.360E+03	1.461E+04	2.777E+04	3.515E+04	3.926E+04	4.492E+04	4.520E+04
Density (g/cm^3)	5.240	5.003	4.107	4.129	4.119	4.219	4.203

Table 12. Predicted Solution Elemental Composition (mole kg^{-1}) and pH in Selected Years for Case 5 (I0Ax2204, I0Bx2022)

Years	99	5332	19989	36145	40827	100030	316900
pH	5.67	6.01	8.45	6.56	5.54	8.08	8.08
Element							
Al	2.173E-11	3.188E-12	8.844E-08	8.243E-08	5.778E-05	6.256E-08	6.253E-08
B	1.195E-03	8.645E-04	3.338E-03	1.239E-05	1.239E-05	1.239E-05	1.239E-05
Ba	2.661E-07	1.992E-07	1.291E-09	2.709E-07	2.371E-07	5.892E-09	5.903E-09
Ca	3.422E-05	2.794E-04	6.494E-05	2.824E-04	4.890E-04	2.424E-04	2.730E-04
Cl	2.014E-04	2.014E-04	2.014E-04	2.014E-04	2.014E-04	2.014E-04	2.014E-04
Cr	5.329E-03	5.326E-03	1.343E-03	1.344E-03	8.087E-02	0.000E+00	0.000E+00
Cu	0.000E+00	0.000E+00	0.000E+00	0.000E+00	1.241E-07	0.000E+00	0.000E+00
F	5.798E-05	1.125E-04	1.295E-04	1.124E-04	2.465E-04	1.143E-04	1.143E-04
Fe	1.039E-11	3.782E-12	1.231E-12	1.850E-12	1.148E-11	1.191E-12	1.191E-12
Gd	0.000E+00	0.000E+00	0.000E+00	0.000E+00	9.635E-11	1.401E-08	1.702E-08
C	4.200E-05	5.165E-05	5.045E-03	9.479E-05	3.956E-05	2.023E-03	2.023E-03
P	7.174E-04	3.260E-06	1.478E-08	2.336E-07	4.532E-05	2.354E-09	1.946E-09
K	3.916E-04	3.306E-04	8.188E-04	1.058E-04	1.252E-04	1.089E-04	1.218E-04
Li	6.915E-06	6.915E-06	6.915E-06	6.915E-06	6.915E-06	6.915E-06	6.915E-06
Mg	1.241E-04	1.294E-04	9.623E-05	9.591E-05	1.918E-04	1.036E-04	9.458E-05
Mn	1.912E-11	3.403E-12	2.180E-16	2.368E-13	6.021E-11	3.159E-16	3.163E-16
Mo	1.071E-04	1.071E-04	1.071E-04	1.071E-04	6.445E-03	0.000E+00	0.000E+00
N	2.488E-04	2.488E-04	1.709E-04	1.709E-04	1.907E-03	1.416E-04	1.416E-04
Na	4.291E-03	3.661E-03	8.367E-03	1.977E-03	1.881E-03	2.042E-03	1.986E-03
Ni	2.498E-03	1.584E-03	4.885E-08	2.162E-04	4.967E-02	2.250E-07	2.256E-07
S	1.219E-03	2.173E-04	2.411E-04	1.954E-04	4.229E-04	1.915E-04	1.915E-04
Si	1.870E-04	1.870E-04	3.607E-05	4.842E-05	6.031E-05	3.595E-05	3.591E-05
Th	0.000E+00	0.000E+00	0.000E+00	0.000E+00	5.222E-14	1.982E-12	1.981E-12
Ti	0.000E+00	0.000E+00	0.000E+00	0.000E+00	3.619E-10	0.000E+00	0.000E+00
U	1.439E-06	1.629E-08	1.458E-05	1.314E-08	4.328E-07	4.245E-07	4.246E-07
Zn	0.000E+00	0.000E+00	0.000E+00	0.000E+00	6.695E-10	0.000E+00	0.000E+00

Case 6a was run with the same first stage as Case 5, but the surface area input for the SNF was decreased by a factor of 10 (Table 10) in the second stage. This change had no significant effect on U and Th loss (Table 10) for Case 6a. Table 13 shows the predicted percent loss of WP components present in the second stage (after ~36,000 years) of Case 6a for selected years. Notice the relatively short persistence of the steel and Al shot WP components compared to the SNF.

Table 13. Predicted % Loss of Shippingport LWBR (Th/U Oxide) SNF WP Components in Selected Years for the Second Stage of Case 6a (l0B$2022)[a]

WP Component	Years		
	40826	100029	316926
	%Loss	%Loss	%Loss
DOE SNF Canister (316L SS)	97.04	100.00	100.00
Inner Basket and Spacer Assembly (316L SS)	100.00	100.00	100.00
Grids (AM350 SS)	100.00	100.00	100.00
EDA II Liner (316NG SS)	65.48	100.00	100.00
ThO_2 Fuel	0.00	0.01	0.07
Low Fissile Binary (Th/U Oxide) Fuel	0.00	0.01	0.07
High Fissile Binary (Th/U Oxide) Fuel	0.00	0.01	0.07
Impact plates (A516 SS)	100.00	100.00	100.00
Al-shot Filler	100.00	100.00	100.00

Source: [a] Spreadsheet "ShipLWBR.xls", sheet "Reactant Losses" (Attachment II).

Table 14 shows the elemental composition of the corrosion products for the second stage of Case 6a. These compositions are nearly identical to those for the second stage of Case 5, except for predicted kg of Th values, which are 10 times lower. There is a small decrease in the predicted kg of U in the second stage of Case 6a, but the bulk of U in the corrosion products has been contributed by HLW glass degradation in the first stage of the run.

Table 15 shows that the amount of U and Th in the WP solution was not affected by the decrease in SNF surface area.

Table 14. Predicted Elemental Composition of Corrosion Products (kg), Total Mass (kg), and Density in Selected Years for Second Stage of Case 6a (l0B$2022)

Years	40827	100030	316930
Element			
O	1.458E+04	1.634E+04	1.649E+04
Al	1.103E+03	1.103E+03	1.103E+03
Ba	2.178E+01	2.173E+01	2.172E+01
Ca	1.383E+02	1.422E+02	1.522E+02
Cr	8.244E+00	7.395E-28	0.000E+00
F	1.764E+00	1.887E+00	1.921E+00
Fe	1.738E+04	2.107E+04	2.107E+04
Gd	7.809E+00	7.809E+00	7.798E+00
H	1.042E+02	1.056E+02	1.075E+02
C	0.000E+00	1.900E+00	1.900E+00
P	1.171E+01	1.077E+01	1.093E+01
K	1.167E+01	1.300E+01	1.479E+01
Mg	6.370E+01	6.322E+01	6.138E+01
Mn	3.705E+02	4.836E+02	4.836E+02
Na	1.004E+01	1.350E+01	1.334E+01
Ni	1.185E+03	1.187E+03	1.187E+03
Si	4.029E+03	4.116E+03	4.230E+03
Th	3.002E-03	4.286E-02	3.075E-01
U	2.357E+02	2.355E+02	2.351E+02
Total mass	3.926E+04	4.492E+04	4.519E+04
Density (g/cm^3)	4.119	4.219	4.203

Table 15. Predicted Solution Elemental Composition (mole kg^{-1}) and pH in Selected Years for the Second Stage of Case 6a (I0B$2022)

Years	40827	100030	316930
pH	5.54	8.08	8.08
Element			
Al	5.778E-05	6.256E-08	6.253E-08
B	1.239E-05	1.239E-05	1.239E-05
Ba	2.371E-07	5.892E-09	5.903E-09
Ca	4.890E-04	2.424E-04	2.730E-04
Cl	2.014E-04	2.014E-04	2.014E-04
Cr	8.087E-02	1.000E-16	1.000E-16
Cu	1.241E-07	1.000E-16	1.000E-16
F	2.465E-04	1.143E-04	1.143E-04
Fe	1.148E-11	1.191E-12	1.191E-12
Gd	9.635E-11	1.401E-08	1.702E-08
C	3.956E-05	2.023E-03	2.023E-03
P	4.532E-05	2.354E-09	1.946E-09
K	1.252E-04	1.089E-04	1.218E-04
Li	6.915E-06	6.915E-06	6.915E-06
Mg	1.918E-04	1.036E-04	9.458E-05
Mn	6.021E-11	3.159E-16	3.163E-16
Mo	6.445E-03	1.000E-16	1.000E-16
N	1.907E-03	1.416E-04	1.416E-04
Na	1.881E-03	2.042E-03	1.986E-03
Ni	4.967E-02	2.250E-07	2.256E-07
S	4.229E-04	1.915E-04	1.915E-04
Si	6.031E-05	3.595E-05	3.591E-05
Th	5.222E-14	1.982E-12	1.981E-12
Ti	3.619E-10	1.000E-16	1.000E-16
U	4.328E-07	4.245E-07	4.246E-07
Zn	6.695E-10	1.000E-16	1.000E-16

Case 6b was similar to Case 6a (surface area input for the SNF was decreased by a factor of 10), but was run with slightly different degradation rates for the HLW glass and Al fill material and different degradation rate constants for SNF (Table 16). The high pH HLW glass degradation rate constant (k_1) in Table 16 is slightly lower than the high pH rate constant (k_1) used for Case 6a (Table 3), while the low pH rate constant (k_2) in Table 16 is higher than the low pH rate constant used for Case 6a (Table 3). This lead to an overall slower rate of HLW glass degradation and a longer first stage (~60,000 years) in Case 6b than in Case 5 or 6a (~36,000 years). Only ~3% of the U from glass degradation was predicted to be lost from the WP in the first stage of Case 6b compared to ~14% predicted U loss in the first stage of Case 5 or 6a (Table 10). This is probably caused by the difference in the highest pH reached during glass degradation in Case 6b (~8.2) than for Case 5 or 6a (pH ~8.5), which leads to lower U solubility (Table 18) and more U in the corrosion products (Table 17). The predicted Gd, U, and Th losses in the second stage of Case 6b are similar to Case 5 or 6a.

Table 16. Special Degradation Rate Constants Used for Case 6b

Reactant	Degradation Rate Constants
HLW Glass	1.983E-18 (k_1) (liter/cm^2·s) 6.144E-11 (k_2) (liter/cm^2·s)
SNF[a]	3.513E-13 (k_1) (liter/cm^2·s) 1.032E-13 (k_2) (liter/cm^2·s)
Al Fill Material	2.288E-13 (mol/cm^2·s)

NOTE: [a]The degradation rate constants for SNF used in Case 6b were based on the following fuel molecular weights (instead of 100g molecular weights used for SNF in the rest of the cases): 264.037 g/mole of thoria fuel; 264.099 g/mole of high fissile binary fuel; and 264.088 g/mole of low fissile binary fuel. So, in effect, the fuel degradation rates for case 6b are the same as the other cases in this calculation—only the rate constants differ.

Table 17. Predicted Elemental Composition of Corrosion Products (kg), Total Mass (kg), and Density for Case 6b (l0Ax2204, l1Ax2204,l0B$2022)

Years	99	30022	59473	62348	101780	316910
Element						
O	2.536E+03	1.087E+04	1.550E+04	1.687E+04	1.705E+04	1.719E+04
Al	7.303E-01	2.491E+02	3.463E+02	1.103E+03	1.103E+03	1.103E+03
Ba	4.380E-02	1.570E+01	2.149E+01	2.148E+01	2.147E+01	2.146E+01
Ca	1.008E+00	1.344E+02	1.685E+02	1.617E+02	1.632E+02	1.714E+02
Cr	0.000E+00	3.962E-16	8.136E+00	8.131E+00	0.000E+00	0.000E+00
F	8.553E-02	1.630E+00	2.604E+00	2.605E+00	2.709E+00	2.742E+00
Fe	5.738E+03	1.436E+04	1.979E+04	2.074E+04	2.107E+04	2.107E+04
Gd	0.000E+00	0.000E+00	0.000E+00	7.809E+00	7.808E+00	7.797E+00
H	1.717E-01	5.576E+01	8.068E+01	1.094E+02	1.098E+02	1.116E+02
C	0.000E+00	1.788E+01	0.000E+00	0.000E+00	1.877E+00	1.877E+00
P	1.145E+00	7.971E+00	1.274E+01	1.485E+01	1.479E+01	1.495E+01
K	1.413E-01	3.523E+01	1.617E+01	1.575E+01	1.578E+01	1.627E+01
Mg	1.760E-01	5.034E+01	5.808E+01	6.451E+01	6.417E+01	6.318E+01
Mn	6.216E+01	2.917E+02	4.459E+02	4.736E+02	4.836E+02	4.836E+02
Na	8.452E-02	2.503E+01	1.394E+01	1.124E+01	1.330E+01	1.427E+01
Ni	1.927E+00	1.049E+03	1.853E+03	1.884E+03	1.883E+03	1.883E+03
S	1.023E-02	1.069E-16	5.091E-18	0.000E+00	0.000E+00	0.000E+00
Si	2.594E+01	2.967E+03	4.468E+03	4.494E+03	4.520E+03	4.633E+03
Th	0.000E+00	0.000E+00	0.000E+00	1.382E-03	3.551E-02	2.980E-01
U	5.655E-01	1.938E+02	2.690E+02	2.690E+02	2.689E+02	2.685E+02
Total Mass	8.368E+03	3.032E+04	4.306E+04	4.625E+04	4.679E+04	4.706E+04
Density (g/cm^3)	5.240	4.244	4.235	4.200	4.206	4.191

Table 18. Predicted Solution Elemental Composition (mole kg^{-1}) and pH in Selected Years for Case 6b (I0Ax2204, I1Ax2204,I0B$2022)

Years	99	30019	59473	62348	101770	316900
pH	5.81	8.19	6.47	5.54	8.08	8.08
Element						
Al	5.675E-12	6.311E-08	5.734E-14	5.480E-05	6.252E-08	6.253E-08
B	1.542E-03	1.750E-03	1.239E-05	1.239E-05	1.239E-05	1.239E-05
Ba	2.669E-07	3.991E-09	2.950E-07	2.363E-07	5.908E-09	5.903E-09
Ca	3.178E-05	2.328E-04	2.863E-04	4.872E-04	2.779E-04	2.781E-04
Cl	2.014E-04	2.014E-04	2.014E-04	2.014E-04	2.014E-04	2.014E-04
Cr	5.606E-03	1.343E-03	1.344E-03	8.085E-02	1.000E-16	1.000E-16
F	5.694E-05	1.213E-04	1.125E-04	4.311E-04	1.000E-16	1.000E-16
Fe	6.574E-12	1.199E-12	2.016E-12	2.373E-04	1.143E-04	1.143E-04
Gd	0.000E+00	0.000E+00	0.000E+00	1.144E-11	1.191E-12	1.191E-12
H	1.110E+02	1.110E+02	1.110E+02	9.488E-11	1.751E-08	1.755E-08
C	4.499E-05	2.727E-03	8.317E-05	3.969E-05	2.022E-03	2.022E-03
P	4.510E-04	2.756E-09	3.267E-07	4.717E-05	1.900E-09	1.884E-09
K	4.624E-04	5.272E-04	1.286E-04	1.505E-04	1.285E-04	1.253E-04
Li	6.915E-06	6.915E-06	6.915E-06	6.915E-06	6.915E-06	6.915E-06
Mg	1.373E-04	1.653E-04	7.814E-05	1.559E-04	1.010E-04	8.753E-05
Mn	1.025E-11	2.621E-16	3.586E-13	5.983E-11	3.165E-16	3.163E-16
Mo	1.291E-04	1.071E-04	1.071E-04	6.444E-03	1.000E-16	1.000E-16
N	2.549E-04	1.709E-04	1.709E-04	1.907E-03	1.416E-04	1.416E-04
Na	4.959E-03	5.372E-03	1.998E-03	1.875E-03	1.957E-03	1.987E-03
Ni	2.292E-03	1.522E-07	1.666E-04	4.927E-02	2.259E-07	2.255E-07
S	1.224E-03	2.193E-04	1.954E-04	4.230E-04	1.915E-04	1.915E-04
Si	1.870E-04	3.567E-05	1.871E-04	6.051E-05	3.585E-05	3.594E-05
Th	0.000E+00	0.000E+00	0.000E+00	4.998E-14	1.981E-12	1.981E-12
Ti	0.000E+00	0.000E+00	0.000E+00	1.326E-06	1.000E-16	1.000E-16
U	1.181E-06	1.421E-06	6.911E-09	4.325E-07	4.250E-07	4.244E-07
Zn	0.000E+00	0.000E+00	0.000E+00	1.932E-06	1.000E-16	1.000E-16

Tables 19 and 20 show the predicted corrosion product and WP solution compositions for Case 7, a two-stage run identical to Case 5 except that hematite was suppressed allowing the precipitation of goethite in the WP. These conditions did not change predicted losses of Th or Gd, but caused slightly higher predicted losses of U from the HLW glass in the first stage (0 through ~32,000 years) and from the SNF in the second stage of Case 7.

If the data in Table 20 are compared to Table 12, we see that the predicted pH is at values near or above 8 for longer periods of time in Case 7. The longer periods of alkaline pH led to higher predicted U solubility and greater predicted U losses from the WP than those predicted for Case 5. The higher density of hematite versus goethite is also reflected in the generally higher corrosion product densities in Table 11 compared to the densities in Table 19.

Table 19. Predicted Elemental Composition of Corrosion Products (kg), Total Mass (kg) and Density in Selected Years for Case 7 (I0Ag2204, I1Ag2204, I0Bg2022)

Years	99	7964	31982	36701	100180	316900
Element						
O	3.354E+03	6.803E+03	1.378E+04	1.565E+04	1.835E+04	1.849E+04
Al	5.801E-01	6.723E+01	3.463E+02	1.102E+03	1.101E+03	1.101E+03
Ba	5.982E-05	3.722E-03	1.025E-02	8.917E-03	7.476E-03	7.430E-03
Ca	9.566E-01	4.004E+01	1.517E+02	1.407E+02	1.377E+02	1.477E+02
Cr	0.000E+00	0.000E+00	0.000E+00	8.265E+00	2.215E-28	0.000E+00
F	8.179E-02	6.455E-01	1.716E+00	1.222E+00	7.795E-01	8.130E-01
Fe	5.737E+03	9.834E+03	1.509E+04	1.667E+04	2.107E+04	2.107E+04
Gd	0.000E+00	0.000E+00	0.000E+00	7.809E+00	7.809E+00	7.799E+00
H	1.035E+02	1.668E+02	2.366E+02	2.921E+02	3.693E+02	3.690E+02
C	0.000E+00	5.875E+00	2.189E+00	0.000E+00	1.898E+00	1.897E+00
P	7.155E-01	3.157E+00	8.395E+00	1.091E+01	5.351E+00	5.512E+00
K	1.015E-01	2.107E+01	1.186E+01	1.134E+01	1.264E+01	1.527E+01
Mg	1.401E-01	2.119E+01	6.407E+01	6.889E+01	6.677E+01	6.495E+01
Mn	6.216E+01	1.761E+02	3.020E+02	3.489E+02	4.836E+02	4.836E+02
Na	6.193E-02	1.248E+01	6.948E+00	6.146E+00	1.475E+01	1.407E+01
Ni	7.879E-01	3.516E+02	1.107E+03	1.146E+03	1.195E+03	1.195E+03
S	8.002E-03	0.000E+00	0.000E+00	0.000E+00	7.229E-16	0.000E+00
Si	2.454E+01	8.131E+02	3.917E+03	3.947E+03	4.048E+03	4.164E+03
Th	0.000E+00	0.000E+00	0.000E+00	5.280E-02	4.657E-01	3.105E+00
U	4.420E-01	5.323E+01	2.262E+02	2.262E+02	2.260E+02	2.255E+02
Total mass	9.260E+03	1.751E+04	3.114E+04	3.549E+04	4.284E+04	4.298E+04
Density (g/cm^3)	4.251	3.897	3.376	3.415	3.521	3.505

Table 20. Predicted Solution Elemental Composition (mole kg^{-1}) and pH in Selected Years for Case 7 (I0Ag2204, I1Ag2204, I0Bg2022)

Years	99	7964	31982	36701	100180	316900
pH	5.67	8.47	7.88	5.27	8.08	8.08
Element						
Al	2.764E-14	8.880E-16	4.104E-08	1.937E-04	6.252E-08	6.247E-08
B	1.199E-03	3.393E-03	1.239E-05	1.239E-05	1.239E-05	1.239E-05
Ba	2.599E-07	1.206E-09	1.672E-08	4.259E-07	5.897E-09	5.915E-09
Ca	3.396E-05	7.708E-05	1.049E-03	1.426E-03	2.345E-04	2.730E-04
Cl	2.014E-04	2.014E-04	2.014E-04	2.014E-04	2.014E-04	2.014E-04
Cr	5.329E-03	1.343E-03	1.343E-03	8.087E-02	0.000E+00	0.000E+00
Cu	0.000E+00	0.000E+00	0.000E+00	3.622E-09	0.000E+00	0.000E+00
F	5.788E-05	1.297E-04	1.123E-04	5.238E-04	1.143E-04	1.143E-04
Fe	3.126E-11	3.730E-12	3.601E-12	6.297E-11	3.598E-12	3.598E-12
Gd	0.000E+00	0.000E+00	0.000E+00	4.829E-10	1.323E-08	1.697E-08
C	4.133E-05	5.221E-03	1.334E-03	3.621E-05	2.021E-03	2.021E-03
P	7.096E-04	1.070E-08	5.672E-10	2.822E-05	2.478E-09	1.949E-09
K	3.922E-04	8.075E-04	1.876E-04	1.946E-04	9.838E-05	1.193E-04
Li	6.915E-06	6.915E-06	6.915E-06	6.915E-06	6.915E-06	6.915E-06
Mg	1.244E-04	4.736E-05	3.876E-04	5.750E-04	9.982E-05	9.520E-05
Mn	1.917E-11	2.193E-16	6.832E-16	2.076E-10	3.161E-16	3.167E-16
Mo	1.071E-04	1.071E-04	1.071E-04	6.445E-03	0.000E+00	0.000E+00
N	2.488E-04	1.709E-04	1.709E-04	1.907E-03	1.416E-04	1.416E-04
Na	4.298E-03	8.660E-03	1.982E-03	1.843E-03	2.075E-03	1.986E-03
Ni	2.487E-03	9.444E-09	1.333E-07	4.691E-02	4.730E-08	4.744E-08
S	1.220E-03	2.419E-04	1.954E-04	4.229E-04	1.915E-04	1.915E-04
Si	1.843E-04	1.045E-04	1.929E-05	3.320E-05	1.971E-05	1.966E-05
Th	0.000E+00	0.000E+00	0.000E+00	2.288E-13	1.981E-12	1.979E-12
Ti	0.000E+00	0.000E+00	0.000E+00	3.592E-10	0.000E+00	0.000E+00
U	1.421E-06	9.937E-06	2.178E-07	7.078E-07	5.725E-07	5.730E-07
Zn	0.000E+00	0.000E+00	0.000E+00	9.305E-10	0.000E+00	0.000E+00

Case 8 was also similar to Case 5 except that the EDA II 316NG stainless steel liner was not included in the EQ6 input file. Table 13 shows that the liner was predicted to persist well into the second stage of Case 6 with the same degradation rates used in Case 8. The large amount of metal in the liner has a significant effect on the composition of WP corrosion products (Table 21) and the chemistry of the WP solution (Table 22). Since steel degradation tends to lower the predicted pH of the WP solution, without the EDA II liner pH values during HLW glass degradation reach a high of 8.7 at ~20,000 years and stay above 8 for the end of the first stage and almost all of the second stage of Case 8 (Table 22). This leads to high (~85%) predicted U losses from HLW glass degradation and slightly higher U and Gd losses in the second stage of Case 8 (Table 10).

Table 21. Predicted Elemental Composition of Corrosion Products (kg), Total Mass (kg), and Density in Selected Years for Case 8 (I0An2204, I0Bn2022)

Years	99	5332	20027	36281	40962	104190	316920
Element							
O	2.524E+03	4.134E+03	9.549E+03	9.972E+03	1.113E+04	1.117E+04	1.130E+04
Al	5.398E-01	2.133E+01	3.361E+02	3.463E+02	1.103E+03	1.103E+03	1.103E+03
B	3.488E-15	2.358E-14	0.000E+00	6.035E-13	0.000E+00	0.000E+00	2.019E-13
Ba	3.191E-02	1.262E+00	2.122E+01	2.187E+01	2.187E+01	2.186E+01	2.186E+01
Ca	9.691E-01	1.215E+01	2.112E+02	2.646E+02	1.878E+02	1.811E+02	1.812E+02
Cr	0.000E+00	4.779E-01	0.000E+00	0.000E+00	8.278E+00	3.270E-26	0.000E+00
Cu	0.000E+00	0.000E+00	0.000E+00	0.000E+00	2.148E+00	2.122E+00	2.038E+00
F	8.422E-02	4.582E-01	9.487E-01	1.045E+00	1.146E+00	1.157E+00	1.190E+00
Fe	5.720E+03	8.282E+03	9.582E+03	9.625E+03	1.040E+04	1.041E+04	1.041E+04
Gd	0.000E+00	0.000E+00	0.000E+00	0.000E+00	7.808E+00	7.802E+00	7.784E+00
H	1.268E-01	4.973E+00	7.111E+01	7.616E+01	1.044E+02	1.049E+02	1.067E+02
C	0.000E+00	3.148E-12	6.874E+01	5.556E+01	1.872E+01	1.816E+01	1.392E+01
P	5.234E-01	2.241E+00	4.640E+00	5.110E+00	7.142E+00	7.196E+00	7.355E+00
K	9.403E-02	2.087E+00	1.171E+02	1.434E+01	1.146E+01	1.172E+01	1.355E+01
Mg	1.344E-01	3.839E+00	1.237E+02	9.464E+01	7.602E+01	7.172E+01	6.664E+01
Mn	6.165E+01	1.344E+02	1.344E+02	1.344E+02	1.567E+02	1.570E+02	1.570E+02
Na	5.793E-02	1.299E+00	8.180E+01	1.103E+01	2.404E+00	1.130E+01	1.229E+01
Ni	2.158E-01	2.026E+02	2.028E+02	2.027E+02	3.218E+02	3.237E+02	3.236E+02
S	7.450E-03	0.000E+00	6.516E-16	0.000E+00	0.000E+00	1.909E-13	0.000E+00
Si	2.390E+01	3.235E+02	3.527E+03	3.908E+03	3.926E+03	3.959E+03	4.071E+03
Th	0.000E+00	0.000E+00	0.000E+00	0.000E+00	4.510E-03	7.705E-01	3.747E+00
U	4.096E-01	1.702E+01	3.377E+01	2.765E+01	2.765E+01	2.756E+01	2.714E+01
Zn	0.000E+00	0.000E+00	0.000E+00	0.000E+00	1.118E+00	8.703E-01	2.907E-01
Total mass	8.333E+03	1.314E+04	2.407E+04	2.476E+04	2.752E+04	2.759E+04	2.782E+04
Density (g/cm^3)	5.241	5.001	3.737	3.717	3.738	3.734	3.720

As would be expected, the predicted density and total mass of corrosion products is less for the second stage of Case 8 (Table 21) than that of Case 5 (Table 11). This is caused by a predicted 50% decrease in the mass of iron oxides formed in the WP, as well as a smaller mass of U, Ni, and Mn precipitated, during Case 8.

Table 22. Predicted Solution Elemental Composition (mole kg^{-1}) and pH in Selected Years for Case 8 (l0An2204, l0Bn2022)

Years	99	5332	20027	36281	40962	104190	316920
pH	5.74	6.15	8.67	8.13	7.33	8.11	8.11
Element							
Al	1.123E-11	9.767E-13	1.181E-07	6.959E-08	1.475E-08	6.740E-08	6.746E-08
B	1.110E-03	7.915E-04	4.231E-03	1.239E-05	1.239E-05	1.239E-05	1.239E-05
Ba	2.414E-07	1.920E-07	4.852E-10	4.828E-09	3.479E-08	5.133E-09	5.120E-09
Ca	2.573E-05	2.865E-04	2.748E-05	2.823E-04	2.517E-02	3.201E-04	3.303E-04
Cl	2.014E-04	2.014E-04	2.014E-04	2.014E-04	2.014E-04	2.014E-04	2.014E-04
Cr	3.986E-03	3.983E-03	0.000E+00	0.000E+00	3.609E-02	0.000E+00	0.000E+00
Cu	0.000E+00	0.000E+00	0.000E+00	0.000E+00	7.377E-07	3.250E-07	3.250E-07
F	5.560E-05	1.136E-04	1.361E-04	1.143E-04	6.083E-05	1.143E-04	1.143E-04
Fe	8.850E-12	3.058E-12	1.287E-12	1.193E-12	1.295E-12	1.192E-12	1.192E-12
Gd	0.000E+00	0.000E+00	0.000E+00	0.000E+00	1.350E-07	2.800E-08	2.964E-08
C	4.333E-05	5.773E-05	8.747E-03	2.258E-03	5.322E-04	2.186E-03	2.188E-03
P	8.077E-04	1.595E-06	4.613E-08	1.790E-09	2.365E-10	1.489E-09	1.394E-09
K	3.725E-04	3.141E-04	9.214E-04	1.428E-04	8.636E-04	1.119E-04	1.211E-04
Li	6.915E-06	6.915E-06	6.915E-06	6.915E-06	6.915E-06	6.915E-06	6.915E-06
Mg	1.185E-04	1.257E-04	3.860E-05	1.959E-04	1.146E-02	1.518E-04	1.208E-04
Mn	1.376E-11	1.772E-12	2.670E-16	2.827E-16	1.504E-14	2.921E-16	2.916E-16
Mo	0.000E+00	0.000E+00	0.000E+00	0.000E+00	2.876E-03	0.000E+00	0.000E+00
N	2.195E-04	2.195E-04	1.416E-04	1.416E-04	9.297E-04	1.416E-04	1.416E-04
Na	4.124E-03	3.518E-03	9.988E-03	1.985E-03	3.182E-03	1.951E-03	1.985E-03
Ni	1.808E-03	8.243E-04	1.794E-08	1.865E-07	1.628E-05	1.977E-07	1.969E-07
S	1.215E-03	2.125E-04	2.496E-04	1.915E-04	2.948E-04	1.915E-04	1.915E-04
Si	1.870E-04	1.871E-04	3.693E-05	3.510E-05	3.490E-05	3.529E-05	3.541E-05
Th	0.000E+00	0.000E+00	0.000E+00	0.000E+00	4.346E-13	2.138E-12	2.140E-12
Ti	0.000E+00	0.000E+00	0.000E+00	0.000E+00	2.953E-10	0.000E+00	0.000E+00
U	1.463E-06	1.061E-08	1.096E-04	6.053E-07	3.902E-08	5.447E-07	5.448E-07
Zn	0.000E+00	0.000E+00	0.000E+00	0.000E+00	1.599E-04	2.194E-06	2.189E-06

Case 9 used a HLW glass composition closer to that in Reference 31 which was simplified only slightly (Ref. 47, Table 5-3) and a different degradation rate than the other cases run in this calculation (Ref. 28, p. 6.5, Fig. 6.2-5). The glass degradation rate was much higher and was not affected by pH changes. These differences shortened the predicted length of the first stage of Case 9 about ten times to ~4000 years. The highest predicted pH of the WP solution during glass degradation was ~9.3 with a high concentration of soluble U (Table 24) and a total loss of U from HLW glass degradation was predicted by ~1200 years (Table 10). Lower pH conditions were predicted for the rest of Case 9 and losses of U, Th, and Gd were minimal during the second stage. Since there was no predicted U in the corrosion products (Table 23) and a very small amount of predicted U loss in the second stage, there was also very little fuel degradation predicted for this case.

Table 23. Predicted Elemental Composition of Corrosion Products (kg), Total Mass (kg), and Density in Selected Years for Case 9 (I0Ao2204,I0Bo2022,I1Bo2022,I2Bo2022)

Years	153	3896	5332	70362	101270	316950
Element						
O	3.231E+03	8.964E+03	1.045E+04	1.527E+04	1.529E+04	1.544E+04
Al	4.358E+01	3.373E+02	1.094E+03	1.093E+03	1.093E+03	1.093E+03
Ba	2.113E+00	1.633E+01	1.633E+01	1.627E+01	1.622E+01	1.622E+01
Ca	1.367E+01	7.379E+01	6.842E+01	7.744E+01	8.370E+01	1.107E+02
Cl	1.224E-13	0.000E+00	0.000E+00	3.017E-01	3.017E-01	3.940E-17
Cr	2.182E-13	8.397E+00	8.397E+00	5.562E+00	0.000E+00	0.000E+00
Cu	2.826E+00	2.045E+01	1.902E+01	0.000E+00	0.000E+00	0.000E+00
F	4.790E-01	1.158E+00	8.997E-01	3.247E-01	6.991E-01	8.938E-01
Fe	5.908E+03	9.250E+03	1.048E+04	2.071E+04	2.071E+04	2.071E+04
Gd	0.000E+00	0.000E+00	7.809E+00	7.809E+00	7.809E+00	7.805E+00
H	7.371E+00	6.444E+01	9.305E+01	9.603E+01	9.623E+01	9.808E+01
C	4.143E+00	6.338E-13	3.661E-13	1.267E-02	1.419E+00	1.929E+00
P	2.343E+00	5.663E+00	7.984E+00	9.739E+00	5.748E+00	5.909E+00
K	2.607E+01	3.396E+01	4.214E+01	3.164E+01	2.981E+01	1.759E+01
Li	2.835E+00	0.000E+00	0.000E+00	0.000E+00	0.000E+00	0.000E+00
Mg	1.560E+01	7.128E+01	7.230E+01	6.823E+01	6.822E+01	6.313E+01
Mn	9.232E+01	3.602E+02	3.957E+02	7.089E+02	7.089E+02	7.089E+02
Na	1.159E+01	8.246E+00	5.525E+00	1.587E+01	1.525E+01	1.173E+01
Ni	2.918E+01	4.449E+02	4.791E+02	5.073E+02	5.066E+02	5.065E+02
Pb	1.139E+00	8.817E+00	8.817E+00	8.817E+00	8.817E+00	8.814E+00
Pu	2.759E-01	2.134E+00	2.133E+00	0.000E+00	0.000E+00	0.000E+00
S	7.084E-12	0.000E+00	2.418E-01	3.349E-01	5.022E-14	1.084E-14
Si	4.298E+02	3.281E+03	3.303E+03	3.493E+03	3.509E+03	3.622E+03
Th	0.000E+00	0.000E+00	9.873E-03	3.566E-01	5.556E-01	3.155E+00
Total mass	9.824E+03	2.295E+04	2.655E+04	4.212E+04	4.215E+04	4.242E+04
Density (g/cm^3)	4.700	3.868	3.874	4.257	4.253	4.237

Table 24. Predicted Solution Elemental Composition (mole kg^{-1}) and pH in Selected Years for Case 9 (I0Ao2204,I0Bo2022,I1Bo2022,I2Bo2022)

Years	153	3896	5332	70362	101270	316950
pH	9.29	6.05	5.43	6.81	8.08	8.08
Element						
Al	9.530E-08	2.230E-06	4.116E-04	5.530E-09	6.280E-08	6.262E-08
B	5.698E-02	1.239E-05	1.239E-05	1.239E-05	1.239E-05	1.239E-05
Ba	7.237E-11	1.930E-07	2.783E-07	1.946E-06	5.807E-09	5.879E-09
Ca	8.756E-06	1.167E-04	1.489E-03	3.363E-05	8.647E-05	2.102E-04
Cl	8.286E-04	2.014E-04	2.014E-04	2.014E-04	2.014E-04	2.014E-04
Cr	5.634E-03	5.329E-03	2.121E-01	1.310E-04	5.092E-15	1.000E-16
Cu	4.444E-06	6.039E-05	2.546E-03	0.000E+00	0.000E+00	0.000E+00
F	3.998E-04	1.114E-04	1.223E-03	5.054E-12	1.143E-04	1.143E-04
Fe	1.839E-12	3.607E-12	1.548E-11	1.544E-12	1.191E-12	1.191E-12
Gd	0.000E+00	0.000E+00	9.381E-10	1.282E-12	2.570E-09	1.108E-08
C	5.382E-02	5.336E-05	3.670E-05	1.392E-04	2.025E-03	2.023E-03
P	1.962E-06	1.315E-05	1.871E-05	8.008E-04	1.232E-08	2.987E-09
K	8.247E-03	3.829E-04	1.564E-03	1.605E-04	2.391E-04	1.656E-04
Li	3.575E-02	6.915E-06	6.915E-06	6.915E-06	6.915E-06	6.915E-06
Mg	9.868E-06	2.469E-04	2.883E-03	4.767E-05	1.105E-04	1.306E-04
Mn	1.028E-15	2.970E-12	1.294E-10	1.130E-13	3.132E-16	3.155E-16
Mo	1.071E-04	1.071E-04	6.427E-03	0.000E+00	0.000E+00	0.000E+00
N	2.488E-04	2.488E-04	4.472E-03	1.416E-04	1.416E-04	1.416E-04
Na	6.934E-02	1.672E-03	3.498E-03	1.452E-03	2.210E-03	1.996E-03
Ni	1.973E-09	2.581E-03	1.105E-01	6.322E-05	2.203E-07	2.248E-07
Np	7.708E-07	1.000E-16	0.000E+00	0.000E+00	0.000E+00	0.000E+00
Pb	3.316E-11	3.196E-10	4.932E-10	2.950E-11	1.953E-09	3.612E-09
Pu	1.053E-07	2.329E-10	4.930E-08	1.293E-08	1.000E-16	1.000E-16
S	9.816E-04	2.056E-04	4.146E-04	8.691E-05	1.915E-04	1.915E-04
Si	5.495E-05	5.368E-05	5.649E-05	4.870E-05	3.647E-05	3.585E-05
Th	0.000E+00	0.000E+00	4.598E-13	1.126E-13	1.990E-12	1.984E-12
Ti	2.391E-03	1.000E-16	5.745E-05	0.000E+00	0.000E+00	0.000E+00
U	1.513E-03	1.000E-16	7.545E-08	4.743E-09	1.073E-07	1.065E-07
Zn	0.000E+00	0.000E+00	7.476E-05	0.000E+00	0.000E+00	0.000E+00

For Case 10, the run conditions for the first stage were low steel degradation rates and high HLW glass degradation rates (VA) with a J-13 water flushing rate of 0.15 m^3/year. The second stage was run with low steel degradation rates, average fuel degradation rate and a J-13 flushing rate of 0.0015 m^3/year. The combination of the low steel degradation rates and high glass degradation rates in the first stage caused predicted pH during HLW glass degradation to be higher (~9.1 at 1000 years) than Cases 5 through 8 in which the high steel degradation rates helped to buffer pH to lower values (Table 26). This high pH increased the amount of soluble U (Table 26) and caused a predicted total loss of U from HLW glass degradation by ~11,000 years. Once the glass had degraded, the predicted pH returned to slightly acid (~6.4) by the end of the first stage at 35,000 years. In the second stage of Case 10, the pH is buffered at pH 5.4 to 5.6 by the degradation of the steels inside the DOE canister, but especially by the degradation of the EDA II liner which was only partially degraded by the end of the run at 317,000 years. The persistent low pH predicted during the second stage of Case 10 is also caused by the low J-13 flushing rate used in this run. The low steel degradation rate and incomplete degradation of the EDA II liner also caused a decrease in the predicted corrosion product densities and total mass as a result of

smaller amounts of Fe, Ni, and Mn precipitated in the WP (Table 25). Very little U was lost from fuel degradation or corrosion product dissolution in the second stage of Case 10.

Table 25. Predicted Elemental Composition of Corrosion Products (kg), Total Mass (kg), and Density in Selected Years for Case 10 (I0Ax1203, I0Bx1021)

Years	1001	34982	53324	106670	317320
Element					
O	3.036E+03	9.098E+03	1.073E+04	1.135E+04	1.305E+04
Al	3.191E+01	3.463E+02	1.103E+03	1.103E+03	1.102E+03
Ba	2.023E+00	2.192E+01	2.192E+01	2.192E+01	2.191E+01
Ca	1.138E+01	1.029E+02	9.745E+01	9.717E+01	9.780E+01
Cr	1.117E-12	8.300E+00	8.299E+00	8.298E+00	8.294E+00
F	2.978E-01	1.057E+00	8.707E-01	6.324E-01	2.003E-01
Fe	5.867E+03	9.355E+03	1.092E+04	1.223E+04	1.583E+04
Gd	0.000E+00	0.000E+00	7.809E+00	7.809E+00	7.809E+00
H	6.586E+00	6.833E+01	9.707E+01	9.745E+01	9.854E+01
C	2.588E+00	2.470E-12	0.000E+00	0.000E+00	0.000E+00
P	1.456E+00	5.169E+00	7.680E+00	8.437E+00	1.028E+01
K	1.700E+01	1.425E+01	1.372E+01	1.353E+01	1.329E+01
Mg	1.143E+01	6.641E+01	7.102E+01	7.038E+01	6.893E+01
Mn	6.219E+01	1.272E+02	1.726E+02	2.129E+02	3.232E+02
N	2.023E-16	1.047E-14	0.000E+00	2.704E-12	3.445E-12
Na	1.253E+01	1.043E+01	7.815E+00	8.278E+00	1.016E+01
Ni	1.011E+01	3.326E+02	3.373E+02	3.415E+02	3.474E+02
S	1.792E-11	2.412E-12	0.000E+00	4.970E-11	6.333E-11
Si	3.216E+02	3.472E+03	3.496E+03	3.519E+03	3.585E+03
Th	0.000E+00	0.000E+00	1.455E-01	5.026E-01	1.729E+00
U	0.000E+00	5.445E-23	2.294E-03	5.968E-03	1.350E-02
Total mass	9.394E+03	2.303E+04	2.709E+04	2.909E+04	3.458E+04
Density (g/cm^3)	4.812	3.809	3.840	3.908	4.061

Table 26. Predicted Solution Elemental Composition (mole kg^{-1}) and pH in Selected Years for Case 10 (I0Ax1203, I0Bx1021)

Years	1001	34982	53324	106670	317320
pH	9.08	6.42	5.41	5.63	5.63
Element					
Al	1.776E-07	2.066E-07	2.341E-04	2.601E-05	2.974E-05
B	2.199E-02	1.239E-05	1.239E-05	1.239E-05	1.239E-05
Ba	1.207E-10	2.466E-07	2.899E-07	2.069E-07	2.068E-07
Ca	1.073E-05	2.042E-04	1.048E-03	2.882E-04	2.843E-04
Cl	2.014E-04	2.014E-04	2.014E-04	2.014E-04	2.014E-04
Cr	1.776E-03	1.777E-03	2.134E-01	4.478E-02	4.478E-02
Cu	0.000E+00	0.000E+00	9.397E-05	5.037E-13	1.000E-16
F	2.252E-04	1.122E-04	7.048E-04	1.603E-04	1.754E-04
Fe	1.548E-12	2.128E-12	1.642E-11	9.023E-12	9.021E-12
Gd	0.000E+00	0.000E+00	4.544E-10	3.626E-11	3.656E-11
C	2.762E-02	7.811E-05	3.613E-05	4.149E-05	4.149E-05
P	5.517E-07	7.392E-07	3.549E-05	5.272E-05	5.287E-05
K	3.535E-03	1.466E-04	2.851E-04	1.505E-04	1.389E-04
Li	6.915E-06	6.915E-06	6.915E-06	6.915E-06	6.915E-06
Mg	1.278E-05	1.717E-04	8.741E-04	2.516E-04	2.130E-04
Mn	6.117E-16	4.593E-13	1.409E-10	3.341E-11	3.339E-11
Mo	3.569E-05	3.569E-05	6.437E-03	3.569E-03	3.569E-03
N	1.773E-04	1.773E-04	4.497E-03	1.120E-03	1.119E-03
Na	4.258E-02	1.933E-03	2.771E-03	1.626E-03	1.874E-03
Ni	3.958E-09	4.146E-04	1.173E-01	2.781E-02	2.773E-02
S	4.986E-04	1.962E-04	7.647E-04	3.197E-04	3.197E-04
Si	4.224E-05	4.960E-05	5.940E-05	5.907E-05	5.930E-05
Th	0.000E+00	0.000E+00	2.589E-13	2.816E-14	3.023E-14
Ti	0.000E+00	0.000E+00	7.505E-06	4.032E-14	1.000E-16
U	5.901E-04	1.000E-16	4.671E-07	4.276E-07	4.289E-07
Zn	0.000E+00	0.000E+00	1.318E-05	7.072E-14	1.000E-16

Cases 15 through 17 and Case 25 were run to examine the effects of different run conditions on U losses from the SNF only. Table 10 shows that only ~2% of the U in the SNF would be lost from the WP with conditions of low steel, high HLW glass (VA), and low fuel degradation rates plus a low J-13 water flushing rate (Case 16). If a high SNF degradation rate is used with these run conditions, then 100% loss of the U from SNF degradation was predicted (Case 17). If average steel, high (Ebert) HLW glass, and the special 25°C fuel degradation rates are combined with the low J-13 flushing rate, a loss of one-third of the U from the SNF was predicted (Case 25).

Tables 27 and 28 show the composition of WP corrosion products and the WP solution during Case 22, a two-stage run showing the effect of high steel degradation rates and high (Ebert) HLW glass rates on WP degradation. Very low predicted pH (~2.3) early in the first stage of this run occured just as the 304L stainless steel GPCs were completely degraded. The high steel

degradation rates caused the complete degradation of all the stainless steel in the first stage (the GPCs, the A516 outer web, and the 316L EDA II liner) by about 2,000 years. Type 304L and 316L stainless steels are very high in Cr (Table 1). As discussed in Assumption 3.7, our calculation assumes the complete oxidation of the Cr released from steel degradation with the consumption of base ($Cr + {}^3/_2O_2 + 2OH^- \leftrightarrow CrO_4^{2-} + H_2O$) which caused the predicted pH in the WP solution to drop. Table 28 shows that the predicted concentration of Cr in the WP solution was higher than any other element at the time of lowest predicted pH. Assuming complete oxidation and release of Mo from the 316L stainless steel in the EDA II liner also produced acid ($2Mo + 3O_2 + 2H_2O \leftrightarrow 2MoO_4^{2-} + 4H^+$). The duration of the very low pH early in Case 22 was not long enough to cause any predicted loss of Gd from the WP (Table 10) during the first stage.

Table 27. Predicted Elemental Composition of Corrosion Products (kg), Total Mass (kg), and Density in Selected Years for Case 22 (I0Ax4404,I1Ax4404,I2Ax4404,I0B$4022)

Years	26	11849	25002	25147	101960	316900
Element						
O	2.122E+03	1.175E+04	1.457E+04	1.604E+04	1.621E+04	1.626E+04
Al	2.427E+00	1.755E+02	3.382E+02	9.881E+02	1.094E+03	1.094E+03
Ba	1.844E-01	1.128E+01	2.183E+01	2.183E+01	2.183E+01	2.182E+01
Ca	0.000E+00	1.318E+02	2.604E+02	1.893E+02	1.768E+02	1.747E+02
Cr	0.000E+00	0.000E+00	0.000E+00	8.265E+00	0.000E+00	0.000E+00
Cu	0.000E+00	0.000E+00	0.000E+00	1.847E+00	2.142E+00	2.122E+00
F	5.551E-12	9.170E-01	1.204E+00	1.222E+00	1.317E+00	1.351E+00
Fe	4.619E+03	1.958E+04	2.025E+04	2.103E+04	2.104E+04	2.104E+04
Gd	0.000E+00	0.000E+00	0.000E+00	6.712E+00	7.803E+00	7.790E+00
H	6.544E-01	3.973E+01	7.488E+01	1.491E+02	1.597E+02	1.570E+02
C	8.702E-10	5.320E+01	6.846E+01	3.718E+01	2.452E+01	1.909E+00
P	7.359E-02	4.485E+00	5.889E+00	7.705E+00	7.981E+00	8.141E+00
K	0.000E+00	5.112E+01	1.242E-17	0.000E+00	0.000E+00	0.000E+00
Mg	0.000E+00	7.174E+01	1.348E+02	1.231E+02	1.151E+02	1.037E+02
Mn	9.830E+01	4.603E+02	4.603E+02	4.826E+02	4.829E+02	4.829E+02
Mo	0.000E+00	0.000E+00	8.311E-29	2.548E+01	1.130E+01	0.000E+00
Na	0.000E+00	4.358E+01	3.791E+00	0.000E+00	1.943E+01	5.785E+01
Ni	0.000E+00	1.960E+01	1.956E+01	1.405E+02	1.405E+02	1.404E+02
S	4.305E-02	0.000E+00	0.000E+00	0.000E+00	0.000E+00	0.000E+00
Si	6.367E+01	2.032E+03	3.784E+03	3.798E+03	3.839E+03	3.952E+03
Th	0.000E+00	0.000E+00	0.000E+00	1.089E-05	7.834E-02	3.183E-01
Ti	0.000E+00	0.000E+00	0.000E+00	1.009E+00	1.174E+00	1.174E+00
U	8.482E-01	0.000E+00	0.000E+00	2.853E-17	0.000E+00	0.000E+00
Zn	0.000E+00	0.000E+00	0.000E+00	1.636E+00	1.870E+00	1.776E+00
Total mass	6.907E+03	3.443E+04	4.000E+04	4.305E+04	4.336E+04	4.351E+04
Density (g/cm^3)	5.300	4.526	4.198	4.109	4.078	4.050

Once all the stainless steel in the first stage was degraded, the predicted WP pH was controlled by dissolution of the HLW glass, and reached a higher maximum value (~8.7) than Case 5 at a much earlier time (~12,000 years vs. ~25,000 years for Case 5). The pH stayed above 8 for the rest of the first stage of Case 22, causing the complete loss of the U from HLW glass degradation. Since the Ebert high HLW glass degradation rate is faster at high pH than the VA high HLW glass degradation rate used for Case 5, predicted complete degradation of the HLW glass occured much sooner in Case 22. After the HLW glass was degraded at about 20,000 years, the pH began to drop and reached a value close to that of the J-13 water (pH ~8.1) by the end of the first stage at 25,000 years.

Table 28. Predicted Solution Elemental Composition (mole kg^{-1}) and pH in Selected Years for Case 22 (I0Ax4404,I1Ax4404,I2Ax4404,I0B$4022)

Years	26	11849	25002	25147	101960	316900
pH	2.28	8.66	8.13	6.92	8.04	8.07
Element						
Al	9.677E-04	9.086E-08	6.825E-08	8.858E-09	7.050E-08	7.495E-08
B	2.207E-02	3.552E-03	1.239E-05	1.239E-05	1.239E-05	1.239E-05
Ba	1.592E-06	5.438E-10	4.839E-09	7.267E-08	7.175E-09	6.179E-09
Ca	1.552E-03	3.114E-05	2.870E-04	2.432E-01	4.231E-04	2.148E-04
Cl	2.014E-04	2.014E-04	2.014E-04	2.014E-04	2.014E-04	2.014E-04
Cr	8.215E-01	1.000E-16	1.000E-16	4.359E-01	1.000E-16	1.000E-16
Cu	0.000E+00	0.000E+00	0.000E+00	3.036E-06	7.877E-08	7.772E-08
F	2.435E-04	1.330E-04	1.143E-04	2.748E-15	1.143E-04	1.143E-04
Fe	8.185E-05	1.216E-12	1.133E-12	1.395E-12	1.130E-12	1.131E-12
Gd	0.000E+00	0.000E+00	0.000E+00	1.481E-09	2.694E-08	1.105E-08
C	2.335E-05	8.265E-03	2.237E-03	3.682E-04	1.844E-03	1.956E-03
P	4.442E-03	3.546E-08	1.640E-09	4.328E-07	1.123E-09	2.819E-09
K	5.826E-03	8.735E-04	1.289E-04	1.289E-04	1.289E-04	1.289E-04
Li	6.915E-06	6.915E-06	6.915E-06	6.915E-06	6.915E-06	6.915E-06
Mg	2.606E-03	3.348E-05	1.672E-04	1.032E-01	2.472E-04	1.255E-04
Mn	8.541E-04	6.533E-16	6.339E-16	4.041E-13	8.288E-16	7.424E-16
Mo	3.357E-03	1.000E-16	1.000E-16	2.716E-06	1.028E-04	1.000E-16
N	1.629E-02	1.416E-04	1.416E-04	1.005E-02	1.416E-04	1.416E-04
Na	4.568E-02	9.326E-03	2.027E-03	2.297E-02	1.401E-03	1.965E-03
Ni	3.898E-01	3.551E-08	3.437E-07	3.042E-04	5.117E-07	4.403E-07
S	3.767E-03	2.402E-04	1.915E-04	1.647E-03	1.915E-04	1.915E-04
Si	1.853E-04	4.691E-05	3.841E-05	3.321E-05	3.734E-05	3.836E-05
Th	0.000E+00	0.000E+00	0.000E+00	1.428E-13	1.461E-12	1.556E-12
U	3.446E-04	9.481E-05	1.000E-16	2.289E-10	9.113E-09	1.025E-08
Zn	0.000E+00	0.000E+00	0.000E+00	9.417E-05	3.691E-07	3.295E-07

The second stage of Case 22 is similar to case 6a; the fuel surface area value was decreased by a factor of 10, but a high rather than moderate stainless steel degradation rate was used. Unlike Case 6a, which began with nearly 35% of the 316L EDA II liner intact, the second stage of Case 22 begins with only the steel in the WP components inside and including the DOE SNF canister. Before 25,200 years, all of this steel has degraded, but the pH is only depressed to 6.9 rather than the value of 5.5 that was reached early in the second stage of Case 6a. The rest of the second stage of Case 22 is similar to Case 6a with very little Gd loss, and no Th or U loss from fuel degradation.

6. RESULTS

This document may be affected by technical product input information that requires confirmation. Any changes to the document that may occur as a result of completing the confirmation activities will be reflected in subsequent revisions. The status of the input information quality may be confirmed by review of the Document Input Reference system database.

A principle objective of this calculation was to assess the chemical characteristics that might lead to the retention of U, Gd, and Th in a WP containing Shippingport LWBR (Th/U oxide) SNF and HLW glass. Twenty-one EQ6 reaction path calculations were carried out to span the range of possible system behavior and to assess the specific and coupled effects of SNF degradation, steel corrosion, HLW glass degradation, and fluid influx rate on U, Gd and Th mobilization. Fluids having a composition of J-13 well water were represented as steady-state reactants with WP components over time spans of up to 317,000 years. Corrosion product accumulation (primarily of iron oxide and smectite) and U, Gd, and Th mobilization were examined as well.

High predicted losses of U (94-95%), mostly from HLW glass degradation, occurred for conditions of low steel degradation rate, high HLW glass degradation rate, and low J-13 water flushing rate (Cases 2, 12, 19 and 20). Total predicted loss of U (from fuel and glass, 6% and 94% of the total moles of U in the WP, respectively) from the WP occurred if a high SNF degradation rate was also used in the run (Cases 3 and 13).

Cases 15 through 17 and Case 25 were run to examine the effects of different run conditions on U losses from the SNF only. Table 10 shows that only ~2% of the U in the SNF would be lost from the WP with conditions of low steel, high HLW glass (VA), and low fuel degradation rates plus a low J-13 water flushing rate (Case 16). If a high SNF degradation rate is used with these run conditions, then 100% loss of the U from SNF degradation was predicted (Case 17). If average steel, high (Ebert) HLW glass, and the 25°C special fuel degradation rates are combined with the low J-13 flushing rate, a loss of one-third of the U from SNF is predicted.

Low, but significant, predicted U losses (5-17%) occurred for conditions of moderate steel degradation rate, and high J-13 water flushing rate (Cases 4, 5, 6a, 7, 14 and 21). These conditions would tend to decrease pH (increase acidity) until the WP steel degrades. Then, the high J-13 flushing rate would prevent build up of alkalinity as HLW glass degradation continued, thus decreasing solubility of U in the WP solution compared with the conditions mentioned above.

Very low predicted U losses (0-4%) occurred for conditions of low steel, low (VA) glass, and low fuel degradation rates, with a high J-13 water flushing rate (Cases 1, 11, 15, and 18). Under these conditions, very little SNF degradation occurred while the EDA II liner and HLW glass also persisted to the end of the runs (~317,000 years), buffering pH to values around 8.1. Uranium mobility was controlled largely by formation of soddyite [$(UO_2)_2(SiO_4)\cdot 2H_2O$]. For these cases, an internal criticality would be possible if the $GdPO_4 \cdot H_2O$, formed by degradation

of the Al fill material, was not well distributed around the remaining SNF and within the WP corrosion products.

Predicted loss of Th from the WP was less than 2% for all the cases run. The predicted amount of Th in solution was controlled to very low levels by formation of the extremely insoluble mineral thorianite (ThO_2). Therefore, this calculation predicts that in times through ~317,000 years most of the Th will remain in the SNF or the WP corrosion products.

Since Gd loss was low (0-4%) for all of the EQ3/6 cases run in this calculation, the risk of a criticality occurring inside the WP seems unlikely if the precipitated $GdPO_4 \cdot H_2O$ is well distributed in the WP corrosion products. For the same reason, an external criticality may be possible under conditions similar to those used to simulate WP degradation in Cases 3, 13, and 17 since all of the U and some Th (0.3 to 1.4 %) in the SNF may be lost from the WP while very little Gd (0 to 0.03%) was predicted to leave the WP in these cases by 317,000 years.

7. REFERENCES

1. Department of Energy (DOE) 1999. *Shippingport LWBR (Th/U Oxide) Fuel Characteristics for Disposal Criticality Analysis.* DOE/SNF/REP-051, Rev. 0. Washington, D.C.: Department of Energy. TIC: 245631.

2. CRWMS M&O 1998. *EQ6 Calculations for Chemical Degradation of Fast Flux Test Facility (FFTF) Waste Packages.* BBA000000-01717-0210-00028 REV 00. Las Vegas, Nevada: CRWMS M&O. ACC: MOL.19981229.0081.

3. CRWMS M&O 1998. "Disruptive Events." Chapter 10 of *Total System Performance Assessment-Viability Assessment (TSPA-VA) Analyses Technical Basis Document.* B00000000-01717-4301-00010 REV 00. Las Vegas, Nevada: CRWMS M&O. ACC: MOL.19980724.0399.

4. CRWMS M&O 1998. *Evaluation of Codisposal Viability for Aluminum-Clad DOE-Owned Spent Fuel: Phase II Degraded Codisposal Waste Package Internal Criticality.* BBA000000-01717-5705-00017 REV 01. Las Vegas, Nevada: CRWMS M&O. ACC: MOL.19981014.0038.

5. National Research Council 1995. *Technical Bases for Yucca Mountain Standards.* Washington, D.C.: National Academy Press. TIC: 217588.

6. LL980711104242.054. Report of the Committee to Review the Use of J-13 Well Water in Nevada Nuclear Waste Storage Investigations. Submittal date: 08/05/1998.

7. DOE (U.S. Department of Energy) 1998. *Total System Performance Assessment.* Volume 3 of *Viability Assessment of a Repository at Yucca Mountain.* DOE/RW-0508. Washington, D.C.: U.S. Department of Energy, Office of Civilian Radioactive Waste Management. ACC: MOL.19981007.0030.

8. Firsching, F.H. and Brune, S.N. 1991. Solubility Products of the Trivalent Rare-Earth Phosphates. *Journal of Chemical Engineering, 36,* 93-95. Washington, D.C.: American Chemical Society. TIC: 240863.

9. Yang, I.C.; Rattray, G.W.; and Yu, P. 1996. *Interpretation of Chemical and Isotopic Data from Boreholes in the Unsaturated Zone at Yucca Mountain, Nevada.* Water Resources Investigations Report 96-4058. Denver, Colorado: U.S. Geological Survey. ACC: MOL.19980528.0216.

10. Weast, R.C. 1977. *CRC Handbook of Chemistry and Physics.* 58th Edition. Pages B-121 and F-210. Cleveland, Ohio: CRC Press. TIC: 242376.

11. CRWMS M&O 1996. *Second Waste Package Probabilistic Criticality Analysis: Generation and Evaluation of Internal Criticality Configurations.* BBA000000-01717-2200-00005 REV 00. Las Vegas, Nevada: CRWMS M&O. ACC: MOL.19960924.0193.

12. CRWMS M&O 1999. *Volumes, Masses, and Surface Areas for Shippingport LWBR Spent Nuclear Fuel in a DOE SNF Canister.* BBA000000-01717-0210-00056 REV 00. Las Vegas, Nevada: CRWMS M&O. ACC: MOL.19991027.0143.

13. Bauccio, M., ed. 1993. *ASM Metals Reference Book.* 3rd Edition. Materials Park, Ohio: ASM International. TIC: 240701.

14. Hillner, E.; Franklin, D.G.; and Smee, J.D. 1998. *The Corrosion of Zircaloy-Clad Fuel Assemblies in a Geologic Repository Environment.* West Mifflin, Pennsylvania: Bettis Atomic Power Laboratory. TIC: 237127.

15. ASME (American Society of Mechanical Engineers) 1998. *1998 ASME Boiler and Pressure Vessel Code.* New York, New York: American Society of Mechanical Engineers. TIC: 247429.

16. Zimmer, E. and Merz, E. 1984. "Dissolution of Thorium-Uranium Mixed Oxides in Concentrated Nitric Acid." *Journal of Nuclear Materials, 124*, 64-67. Amsterdam, The Netherlands: Elsevier Science Publishers. TIC: 247214.

17. CRWMS M&O 1999. *Addendum to: EQ6 Computer Program for Theoretical Manual, Users Guide, & Related Documentation.* Software Change Request (SCR) LSCR198. UCRL-MA-110662 PT IV. Las Vegas, Nevada: CRWMS M&O. ACC: MOL.19990305.0112.

18. CRWMS M&O 1998. *Software Qualification Report (SQR) Addendum to Existing LLNL Document UCRL-MA-110662 PT IV: Implementation of a Solid-Centered Flow-Through Mode for EQ6 Version 7.2B. CSCI: UCRL-MA-110662 V 7.2b. SCR: LSR198.* Las Vegas, Nevada: CRWMS M&O. ACC: MOL.19990920.0169.

19. CRWMS M&O 1998. *EQ6 Calculations for Chemical Degradation of Pu-Ceramic Waste Packages.* BBA000000-01717-0210-00018 REV 00. Las Vegas, Nevada: CRWMS M&O. ACC: MOL.19980918.0004.

20. CRWMS M&O 1998. *EQ3/6 Software Installation and Testing Report for Pentium Based Personal Computers (PCs).* CSCI: LLYMP9602100. Las Vegas, Nevada: CRWMS M&O. ACC: MOL.19980813.0191.

21. CRWMS M&O 1999. *EQ6 Calculations for Chemical Degradation of TRIGA Codisposal Waste Packages.* CAL-EDC-MD-000001 REV 00. Las Vegas, Nevada: CRWMS M&O. ACC: MOL.19991118.0050.

22. Wolery, T.J. 1992. *EQ3/6, A Software Package for Geochemical Modeling of Aqueous Systems. Package Overview and Installation Guide (Version 7.0).* UCRL-MA-110662 PT I. Livermore, California: Lawrence Livermore National Laboratory. TIC: 205087.

23. Daveler, S.A. and Wolery, T.J. 1992. *EQPT, A Data File Preprocessor for the EQ3/6 Software Package. User's Guide, and Related Documentation (Version 7.0).* UCRL-MA-110662 PT II. Livermore, California: Lawrence Livermore National Laboratory. TIC: 205240.

24. Wolery, T.J. 1992. *EQ3NR, A Computer Program for Geochemical Aqueous Speciation-Solubility Calculations. Theoretical Manual, User's Guide, and Related Documentation (Version 7.0).* UCRL-MA-110662 PT III. Livermore, California: Lawrence Livermore National Laboratory. TIC: 205154.

25. Wolery, T.J. and Daveler, S.A. 1992. *EQ6, A Computer Program for Reaction Path Modeling of Aqueous Geochemical Systems: Theoretical Manual, User's Guide, and Related Documentation (Version 7.0).* UCRL-MA-110662 PT IV. Livermore, California: Lawrence Livermore National Laboratory. TIC: 205002.

26. Spahiu, K. and Bruno, J. 1995. *A Selected Thermodynamic Database for REE to be Used in HLNW Performance Assessment Exercises.* SKB Technical Report 95-35. Stockholm, Sweden: Swedish Nuclear Fuel and Waste Management Company. TIC: 225493.

27. CRWMS M&O 1998. *EQ6 Calculations for Chemical Degradation of PWR LEU and PWR MOX Spent Fuel Waste Packages.* BBA000000-01717-0210-00009 REV 00. Las Vegas, Nevada: CRWMS M&O. ACC: MOL.19980701.0483.

28. CRWMS M&O 1995. *Total System Performance Assessment - 1995: An Evaluation of the Potential Yucca Mountain Repository.* B00000000-01717-2200-00136 REV 01. Las Vegas, Nevada: CRWMS M&O. ACC: MOL.19960724.0188.

29. McCright, R.D. 1998. *Corrosion Data and Modeling, Update for Viability Assessment.* Volume 3 of *Engineered Materials Characterization Report.* UCRL-ID-119564, Rev. 1.1. Livermore, California: Lawrence Livermore National Laboratory. ACC: MOL.19980806.0177.

30. CRWMS M&O 2000. *Waste Package Degradation Process Model Report.* TDR-WIS-MD-000002 REV 00. Las Vegas, Nevada: CRWMS M&O. ACC: MOL.20000328.0322.

31. CRWMS M&O 1999. *DOE SRS HLW Glass Chemical Composition.* BBA000000-01717-0210-00038 REV 00. Las Vegas, Nevada: CRWMS M&O. ACC: MOL.19990215.0397.

32. CRWMS M&O 1999. *EQ6 Calculation for Chemical Degradation of Pu-Ceramic Waste Packages: Effects of Updated Materials Composition and Rates.* CAL-EDC-MD-000003 REV 00. Las Vegas, Nevada: CRWMS M&O. ACC: MOL.19990928.0235.

33. DOE (U.S. Department of Energy) 1992. *Characteristics of Potential Repository Wastes.* DOE/RW-0184-R1. Volume 1. Washington, D.C.: U.S. Department of Energy, Office of Civilian Radioactive Waste Management. ACC: HQO.19920827.0001.

34. CRWMS M&O 1998. "Waste Form Degradation, Radionuclide Mobilization, and Transport Through the Engineered Barrier System." Chapter 6 of *Total System Performance Assessment-Viability Assessment (TSPA-VA) Analyses Technical Basis Document.* B00000000-01717-4301-00006 REV 01. Las Vegas, Nevada: CRWMS M&O. ACC: MOL.19981008.0006.

35. CRWMS M&O 2000. *Defense High Level Waste Glass Degradation.* ANL-EBS-MD-000016 REV 00. Las Vegas, Nevada: CRWMS M&O. ACC: MOL.20000329.1183.

36. CRWMS M&O. 2000. *DSNF and Other Waste Form Degradation Abstraction.* ANL-WIS-MD-000004 REV 00 . Las Vegas, Nevada: CRWMS M&O. ACC: MOL.20000223.0502.

37. Osthols, E. and Malmström, M. 1995. "Dissolution Kinetics of ThO_2 in Acid and Carbonate Media." *Radiochimica Acta, 68,* (2), 113-119. München, Germany: R. Oldenbourg Verlag. TIC: 245120.

38. Hollingsworth, E.H. and Hunsicker, H.Y. 1987. "Corrosion of Aluminum and Aluminum Alloys." Volume 13 of *Metals Handbook* . 9th Edition.. Pages 583-609. Metals Park, Ohio: ASM International. TIC: 209807.

39. CRWMS M&O 1998. "Unsaturated Zone Hydrology Model." Chapter 2 of *Total System Performance Assessment-Viability Assessment (TSPA-VA) Analyses Technical Basis Document.* B00000000-01717-4301-00002 REV 01. Las Vegas, Nevada: CRWMS M&O. ACC: MOL.19981008.0002.

40. ASTM A 20/A 20M-95a. 1995. *Standard Specification for General Requirements for Steel Plates for Pressure Vessels.* West Conshohocken, Pennsylvania: American Society for Testing and Materials. TIC: 240026.

41. DOE (U.S. Department of Energy) 2000. *Quality Assurance Requirements and Description.* DOE/RW-0333P, Rev. 10. Washington, D.C.: U.S. Department of Energy, Office of Civilian Radioactive Waste Management. ACC: MOL.20000427.0422.

42. Roberts, W.L.; Rapp, G.R., Jr.; and Weber, J. 1974. *Encyclopedia of Minerals.* Pages 172, 240, 241, 413, 500, 689, and 690. New York, New York: Van Nostrand Reinhold. TIC: 238571.

43. Audi, G. and Wapstra A.H. 1995. *Atomic Mass Adjustment: Mass List for Analysis.* Upton, New York: Brookhaven National Laboratory, National Nuclear Data Center. TIC: 242718.

44. Walker, F.W.; Parrington, J.R.; and Feiner, F. 1989. *Nuclides and Isotopes.* 14th Edition. San Jose, California: General Electric Company. TIC: 201637.

45. Lee, J.H. and Byrne, R.H. 1992. "Examination of Comparative Rare Earth Element Complexation Behavior Using Linear Free-Energy Relationships." *Geochimica et Cosmochimica Acta, 56*, 1127-1137. New York, New York: Pergamon Press. TIC: 240861.

46. CRWMS M&O 1998. *Disposal Criticality Analysis Methodology Topical Report.* B00000000-01717-5705-00095 REV 00. Las Vegas, Nevada: CRWMS M&O. ACC: MOL.19980918.0005.

47. CRWMS M&O 1999. *EQ6 Calculation for Chemical Degradation of Shippingport PWR (HEU Oxide) Spent Nuclear Fuel Waste Packages.* CAL-EDC-MD-000002 REV 00. Las Vegas, Nevada: CRWMS M&O. ACC: MOL.19991220.0322.

48. AP-SI.1Q, Rev. 2, ICN 4. *Software Management.* Washington, D.C.: U.S. Department of Energy, Office of Civilian Radioactive Waste Management. ACC: MOL.20000223.0508.

49. CRWMS M&O 1997. *Criticality Evaluation of Degraded Internal Configurations for the PWR AUCF WP Designs.* BBA000000-01717-0200-00056 REV 00. Las Vegas, Nevada: CRWMS M&O. ACC: MOL.19971231.0251.

50. AP-3.12Q, Rev.0, ICN 2. *Calculations.* Washington, D.C.: U.S. Department of Energy, Office of Civilian Radioactive Waste Management. ACC: MOL.20000620.0068.

51. CRWMS M&O 2000. *DOE SNF Analysis Plan for FY 2000.* Development Plan TDP-EDC-MD-000003 REV 01. Las Vegas, Nevada: CRWMS M&O. ACC: MOL.20000510.0169.

52. AP-SV.1Q, Rev. 0, ICN 2. *Control of the Electronic Management of Information.* Washington, D.C.: U.S. Department of Energy, Office of Civilian Radioactive Waste Management. ACC: MOL.20000831.0065.

53. CRWMS M&O 2000. Process Control Evaluation for Supplement V: (DOE SNF Analysis Plan for FY 2000 (TPDP) TDP-EDC-MD-000003 REV 01). Las Vegas, Nevada: CRWMS M&O. ACC: MOL.20000718.0187.

54. ASTM A 516/A 516M - 90. 1991. *Standard Specification for Pressure Vessel Plates, Carbon Steel, for Moderate- and Lower-Temperature Service.* Philadelphia, Pennsylvania: American Society for Testing and Materials. TIC: 240032.

55. ASTM G 1-90 (Reapproved 1999). 1990. *Standard Practice for Preparing, Cleaning, and Evaluating Corrosion Test Specimens.* West Conshohocken, Pennsylvania: American Society for Testing and Materials. TIC: 238771.

56. ASTM A 276-91a. 1991. *Standard Specification for Stainless and Heat-Resisting Steel Bars and Shapes.* Philadelphia, Pennsylvania: American Society for Testing and Materials. TIC: 240022.

57. ASTM A 240/A 240M-94b. 1994. *Standard Specification for Heat-Resisting Chromium and Chromium-Nickel Stainless Steel Plate, Sheet, and Strip for Pressure Vessels.* Philadelphia, Pennsylvania: American Society for Testing and Materials. TIC: 240020.

58. Baxter, R. G. 1988. *Defense Waste Processing Facility Wasteform and Canister Description.* DP-1606, Rev. 2. Aiken, South Carolina: Savannah River Plant. TIC: 8704.

59. Weast, R.C., ed. 1979. *CRC Handbook of Chemistry and Physics.* 60th Edition, 1979 - 1980. Boca Raton, Florida: CRC Press. TIC: 245312.

60. MO0006J13WTRCM.000. Recommended Mean Values of Major Constituents in J-13 Well Water. Submittal date: 06/07/2000. Submit to RPC URN-0532

8. ATTACHMENTS

ATTACHMENT I. LIST OF FILES ON ATTACHED COMPACT DISCS (CDS).

ATTACHMENT II. NINE CDS.

ATTACHMENT I. LIST OF FILES ON ATTACHED COMPACT DISCS (CDs)

This attachment contains file listings of the CDs attached to this calculation.

Following file types are included in Tables I-1 to I-9:

1. Excel spreadsheets (extension = xls), called out in the text and tables;
2. EQ6 input files (extension = 6i), as discussed in Section 5.3.1, have 8-character names L???????.6i;
3. EQ6 output files (text, extension = 6o);
4. Tab-delimited text files (extension = txt), with names L???????.elem????.txt. as discussed in Section 5.3.2; these contain total aqueous moles (*.elem_aqu.txt), total moles in minerals, aqueous phase, and remaining special reactants (*.elem_tot.txt), and the total moles in minerals alone (*.elem_min.txt). The *.elem_tot.txt and *.elem_min.txt also have the volume in cm^3 of the minerals and total solids (including special reactants) in the system;
5. MS-DOS/Win95/Win98 executables (extension = exe) for the version of EQ6 and runeq6 used in the calculations; and
6. EQ6 data files used for the calculations, with the text file data0.nuc or data0.ymp and the binary versions data1.nuc and data1.ymp, respectively.

Table I-1. Contents of CD SLWBR1

Filename	File Size (bytes)	Date	Time
l0&x1113.6o	7,365,016	05/03/2000	8:04pm
l0&x1113.6p	51,186	05/03/2000	8:04pm
L0&x1113.bin	70,311,984	05/03/2000	8:04pm
L0&X1113.TXT	13,219	05/08/2000	3:45pm
L0&x1113.6i	50,368	05/03/2000	4:44pm
L0&x1113.elem_aqu.txt	56,193	05/03/2000	8:04pm
L0&x1113.elem_min.txt	52,912	05/03/2000	8:04pm
L0&x1113.elem_tot.txt	52,925	05/03/2000	8:04pm
L0&x1211.6i	50,224	04/12/2000	4:06pm
l0&x1211.6o	3,329,006	04/13/2000	3:22pm
l0&x1211.6p	50,890	04/13/2000	3:22pm
L0&x1211.bin	7,107,504	04/13/2000	3:22pm
L0&X1211.TXT	12,986	05/09/2000	11:49am
L0&x1231.bin	2,279,752	05/03/2000	8:36pm
L0&x1231.6i	50,278	05/03/2000	4:00pm
l0&x1231.6o	1,593,684	05/03/2000	8:37pm
l0&x1231.6p	51,902	05/03/2000	8:37pm
L0&X1231.TXT	4,286	05/09/2000	12:04pm
L0&x1231.elem_aqu.txt	13,248	05/03/2000	8:36pm
L0&x1231.elem_min.txt	12,487	05/03/2000	8:36pm
L0&x1231.elem_tot.txt	12,500	05/03/2000	8:36pm
L0&x1211.elem_aqu.txt	28,381	04/13/2000	3:22pm
L0&x1211.elem_min.txt	26,732	04/13/2000	3:22pm
L0&x1211.elem_tot.txt	26,745	04/13/2000	3:22pm
l00g1113.6p	50,778	05/03/2000	6:40pm
L00g1113.bin	70,335,768	05/03/2000	6:40pm

Table I-1. Contents of CD SLWBR1 (Continued)

Filename	File Size (bytes)	Date	Time
l00g1113.6o	7,437,529	05/03/2000	6:40pm
L00G1113.TXT	13,219	05/08/2000	1:58pm
L00g1113.6i	50,200	05/03/2000	4:57pm
L00g1113.elem_aqu.txt	57,011	05/03/2000	6:40pm
L00g1113.elem_min.txt	53,682	05/03/2000	6:40pm
L00g1113.elem_tot.txt	53,695	05/03/2000	6:40pm
L00g1211.6i	50,302	05/03/2000	4:10pm
l00g1211.6o	315,673	05/03/2000	8:30pm
l00g1211.6p	51,538	05/03/2000	8:30pm
L00g1211.bin	221,016	05/03/2000	8:30pm
L00G1211.TXT	517	05/09/2000	11:26am
L00g1211.elem_aqu.txt	2,205	05/03/2000	8:30pm
L00g1211.elem_min.txt	2,092	05/03/2000	8:30pm
L00g1211.elem_tot.txt	2,105	05/03/2000	8:30pm
l01x1211.6i	44,872	05/04/2000	10:20am
L01X1211.TXT	7,552	05/09/2000	9:31am
L01x1211.bin	4,915,328	05/04/2000	1:37pm
l01x1211.6o	1,854,758	05/04/2000	1:37pm
l01x1211.6p	43,878	05/04/2000	1:37pm
L01x1231.bin	4,307,352	05/03/2000	8:34pm
l01x1231.6o	1,383,429	05/03/2000	8:34pm
l01x1231.6i	40,982	05/03/2000	3:43pm
l01x1231.6p	39,994	05/03/2000	8:34pm
L01X1231.TXT	2,846	05/08/2000	6:17pm
L01x1211.elem_min.txt	15,090	05/04/2000	1:37pm
L01x1211.elem_tot.txt	15,103	05/04/2000	1:37pm
L01x1211.elem_aqu.txt	16,043	05/04/2000	1:37pm
L01x1231.elem_min.txt	12,447	05/03/2000	8:34pm
L01x1231.elem_tot.txt	12,460	05/03/2000	8:34pm
L01x1231.elem_aqu.txt	13,256	05/03/2000	8:34pm
L02G1211.TXT	2,732	05/09/2000	11:27am
L02g1211.bin	1,450,840	05/05/2000	3:23pm
l02g1211.6i	39,839	05/05/2000	3:20pm
l02g1211.6o	489,421	05/05/2000	3:23pm
l02g1211.6p	39,425	05/05/2000	3:23pm
l02g1231.6i	36,047	05/05/2000	11:16am
l02g1231.6o	357,218	05/05/2000	2:33pm
l02g1231.6p	35,393	05/05/2000	2:33pm
L02G1231.TXT	1,014	05/09/2000	9:50am
L02g1231.bin	1,086,568	05/05/2000	2:33pm
L02g1211.elem_min.txt	4,144	05/05/2000	3:23pm
L02g1211.elem_tot.txt	4,157	05/05/2000	3:23pm
L02g1211.elem_aqu.txt	4,401	05/05/2000	3:23pm
L02g1231.elem_min.txt	3,317	05/05/2000	2:33pm
L02g1231.elem_tot.txt	3,330	05/05/2000	2:33pm
L02g1231.elem_aqu.txt	3,526	05/05/2000	2:33pm
l0@x1211.6o	1,744,131	05/03/2000	8:30pm
l0@x1211.6p	52,098	05/03/2000	8:30pm
L0@x1211.bin	2,667,824	05/03/2000	8:30pm
L0@X1211.TXT	4,217	05/09/2000	11:05am
L0@x1211.6i	50,334	05/03/2000	4:28pm
L0@x1211.elem_min.txt	13,662	05/03/2000	8:30pm
L0@x1211.elem_tot.txt	13,675	05/03/2000	8:30pm

Table I-1. Contents of CD SLWBR1 (Continued)

Filename	File Size (bytes)	Date	Time
L0@x1231.elem_aqu.txt	30,890	05/03/2000	8:43pm
L00g1231.6i	50,287	05/03/2000	4:05pm
l00g1231.6o	315,639	05/03/2000	8:33pm
l00g1231.6p	51,500	05/03/2000	8:33pm
L00g1231.bin	221,016	05/03/2000	8:33pm
L00G1231.TXT	517	05/09/2000	9:48am
L00g1231.elem_aqu.txt	2,205	05/03/2000	8:33pm
L00g1231.elem_min.txt	2,092	05/03/2000	8:33pm
L00g1231.elem_tot.txt	2,105	05/03/2000	8:33pm
l00x1211.6o	1,593,698	05/03/2000	8:32pm
l00x1211.6p	51,792	05/03/2000	8:32pm
L00x1211.bin	2,279,752	05/03/2000	8:32pm
L00X1211.TXT	4,286	05/09/2000	9:31am
L00x1211.6i	50,231	05/03/2000	4:08pm
L00x1231.6i	50,213	04/13/2000	5:55pm
l00x1231.6o	1,872,153	04/13/2000	6:04pm
l00x1231.6p	51,508	04/13/2000	6:04pm
L00x1231.bin	2,678,016	04/13/2000	6:04pm
L00X1231.TXT	5,011	05/08/2000	6:15pm
L00x1231.elem_min.txt	14,797	04/13/2000	6:04pm
L00x1211.elem_aqu.txt	13,248	05/03/2000	8:32pm
L00x1211.elem_min.txt	12,487	05/03/2000	8:32pm
L00x1211.elem_tot.txt	12,500	05/03/2000	8:32pm
L00x1231.elem_aqu.txt	15,702	04/13/2000	6:04pm
L00x1231.elem_tot.txt	14,810	04/13/2000	6:04pm
l01g1211.6o	2,888,358	05/04/2000	6:41pm
l01g1211.6p	51,490	05/04/2000	6:41pm
L01g1211.bin	5,717,888	05/04/2000	6:41pm
L01G1211.TXT	10,521	05/09/2000	11:25am
l01g1211.6i	51,758	05/04/2000	4:51pm
L01g1211.elem_aqu.txt	25,109	05/04/2000	6:41pm
L01g1211.elem_min.txt	23,652	05/04/2000	6:41pm
L01g1211.elem_tot.txt	23,665	05/04/2000	6:41pm
l01g1231.6p	51,304	05/04/2000	6:45pm
l01g1231.6i	51,648	05/04/2000	4:36pm
l01g1231.6o	2,911,973	05/04/2000	6:45pm
L01g1231.bin	5,765,584	05/04/2000	6:45pm
l0@x1231.6o	3,605,604	05/03/2000	8:43pm
L0@x1231.6i	50,438	04/12/2000	3:59pm
l0@x1231.6p	51,088	05/03/2000	8:43pm
L0@x1231.bin	8,027,088	05/03/2000	8:43pm
L0@X1231.TXT	12,168	05/08/2000	8:25am
L0@x1211.elem_aqu.txt	14,471	05/03/2000	8:30pm
L0@x1231.elem_min.txt	29,145	05/03/2000	8:43pm
L0@x1231.elem_tot.txt	29,158	05/03/2000	8:43pm
l1&x1113.6i	40,737	05/04/2000	5:06pm
L1&x1113.bin	307,391,304	05/04/2000	6:32pm
L1&X1113.TXT	58,188	05/08/2000	3:44pm
l1&x1113.6o	30,698,800	05/04/2000	6:32pm
l1&x1113.6p	40,247	05/04/2000	6:32pm
L1&x1113.elem_min.txt	203,294	05/04/2000	6:32pm
L1&x1113.elem_tot.txt	203,307	05/04/2000	6:32pm
L1&x1113.elem_aqu.txt	217,255	05/04/2000	6:32pm
l1&x1231.6i	44,982	05/04/2000	10:09am

Table I-1. Contents of CD SLWBR1 (Continued)

Filename	File Size (bytes)	Date	Time
L1&x1231.bin	5,945,408	05/04/2000	1:44pm
I1&x1231.6o	2,009,287	05/04/2000	1:44pm
L1&X1231.TXT	9,099	05/09/2000	11:59am
I1&x1231.6p	43,988	05/04/2000	1:44pm
L1&x1231.elem_min.txt	16,582	05/04/2000	1:44pm
L1&x1231.elem_tot.txt	16,595	05/04/2000	1:44pm
L1&x1231.elem_aqu.txt	17,631	05/04/2000	1:44pm
L1@x1211.bin	4,882,136	05/04/2000	1:31pm
I1@x1211.6o	1,706,534	05/04/2000	1:31pm
I1@x1211.6i	45,178	05/04/2000	10:31am
L1@X1211.TXT	7,553	05/09/2000	11:08am
I1@x1211.6p	44,026	05/04/2000	1:31pm
L1@x1211.elem_min.txt	13,971	05/04/2000	1:31pm
L1@x1211.elem_tot.txt	13,984	05/04/2000	1:31pm
L1@x1211.elem_aqu.txt	14,852	05/04/2000	1:31pm
L01G1231.TXT	10,666	05/09/2000	9:49am
L01g1231.elem_aqu.txt	25,518	05/04/2000	6:45pm
L01g1231.elem_min.txt	24,037	05/04/2000	6:45pm
L01g1231.elem_tot.txt	24,050	05/04/2000	6:45pm

Table I-2. Contents of CD SLWBR2

File Name	File Size (bytes)	Date	Time
L0&x2133.6i	50,225	04/12/2000	3:58pm
L0&x2133.bin	317,937,504	05/03/2000	11:39pm
l0&x2133.6o	30,593,046	05/03/2000	11:40pm
l0&x2133.6p	50,972	05/03/2000	11:40pm
L0&X2133.TXT	69,750	05/09/2000	12:23pm
L0&x2133.elem_min.txt	217,307	05/03/2000	11:39pm
L0&x2133.elem_tot.txt	217,320	05/03/2000	11:39pm
L0&x2133.elem_aqu.txt	230,836	05/03/2000	11:39pm
L00g2133.6i	50,209	04/13/2000	5:58pm
L00g2133.bin	83,179,632	04/13/2000	6:31pm
l00g2133.6o	8,702,624	04/13/2000	6:31pm
l00g2133.6p	50,778	04/13/2000	6:31pm
L00G2133.TXT	18,322	05/08/2000	6:27pm
L00g2133.elem_min.txt	62,922	04/13/2000	6:31pm
L00g2133.elem_tot.txt	62,935	04/13/2000	6:31pm
L00g2133.elem_aqu.txt	66,827	04/13/2000	6:31pm
L00x1113.6i	50,201	05/03/2000	4:42pm
L00X1113.TXT	13,219	05/08/2000	6:04pm
L00x1113.bin	70,319,904	05/03/2000	8:26pm
l00x1113.6o	7,364,912	05/03/2000	8:26pm
l00x1113.6p	50,852	05/03/2000	8:26pm
L00x1113.elem_min.txt	52,912	05/03/2000	8:26pm
L00x1113.elem_tot.txt	52,925	05/03/2000	8:26pm
L00x1113.elem_aqu.txt	56,193	05/03/2000	8:26pm
l1&x2133.6i	38,920	05/04/2000	9:58am
L1&x2133.bin	82,796,880	05/04/2000	3:28pm
l1&x2133.6o	8,551,109	05/04/2000	3:28pm
L1&X2133.TXT	16,426	05/09/2000	12:25pm
l1&x2133.6p	37,868	05/04/2000	3:28pm
L1&x2133.elem_min.txt	53,807	05/04/2000	3:28pm
L1&x2133.elem_tot.txt	53,820	05/04/2000	3:28pm
L1&x2133.elem_aqu.txt	57,760	05/04/2000	3:28pm

Table I-3. Contents of CD SLWBR3

File Name	File Size (bytes)	Date	Time
L00x2133.bin	158,897,456	05/04/2000	12:31am
L00X2133.TXT	35,006	05/09/2000	12:34pm
L00x2133.6i	50,163	04/12/2000	3:57pm
l00x2133.6o	15,962,998	05/04/2000	12:31am
l00x2133.6p	50,824	05/04/2000	12:31am
L00x2133.elem_min.txt	114,897	05/04/2000	12:31am
L00x2133.elem_tot.txt	114,910	05/04/2000	12:31am
L00x2133.elem_aqu.txt	122,042	05/04/2000	12:31am
l01x2133.6i	38,772	05/04/2000	10:03am
l01x2133.6o	22,457,467	05/04/2000	4:15pm
l01x2133.6p	37,720	05/04/2000	4:15pm
L01x2133.bin	219,457,376	05/04/2000	4:14pm
L01X2133.TXT	43,292	05/09/2000	12:35pm
L01x2133.elem_min.txt	140,257	05/04/2000	4:14pm
L01x2133.elem_tot.txt	140,270	05/04/2000	4:14pm
L01x2133.elem_aqu.txt	150,594	05/04/2000	4:14pm
L0AX4404.TXT	1,387	06/02/2000	5:35pm
L0AX4404.bin	1,368,688	06/08/2000	12:21pm
L0Ax4404.6i	39,618	06/08/2000	11:49am
l0ax4404.6o	535,811	06/08/2000	12:21pm
l0ax4404.6p	37,873	06/08/2000	12:21pm
L0AX4404.elem_min.txt	5,057	06/08/2000	12:21pm
L0AX4404.elem_tot.txt	5,070	06/08/2000	12:21pm
L0AX4404.elem_aqu.txt	5,410	06/08/2000	12:21pm
L1AX4404.TXT	775	06/02/2000	5:36pm
L1AX4404.bin	706,184	06/08/2000	12:22pm
l1ax4404.6i	35,205	06/08/2000	11:51am
l1ax4404.6o	248,070	06/08/2000	12:22pm
l1ax4404.6p	35,419	06/08/2000	12:22pm
L1AX4404.elem_min.txt	2,457	06/08/2000	12:22pm
L1AX4404.elem_tot.txt	2,470	06/08/2000	12:22pm
L0@X3441.TXT	3,524	06/01/2000	12:17pm
L0@x3441.6i	50,253	05/30/2000	1:05pm
L0@x3441.bin	240,008	05/30/2000	1:55pm
l0@x3441.6o	272,096	05/30/2000	1:55pm
l0@x3441.6p	50,023	05/30/2000	1:55pm
L0@x3441.elem_min.txt	2,149	05/30/2000	1:55pm
L0@x3441.elem_tot.txt	2,162	05/30/2000	1:55pm
L0@x3441.elem_aqu.txt	2,262	05/30/2000	1:55pm
L1@X3441.TXT	15,824	06/01/2000	12:15pm
L1@x3441.bin	8,577,424	05/30/2000	2:43pm
l1@x3441.6o	2,966,117	05/30/2000	2:43pm
l1@x3441.6p	51,073	05/30/2000	2:43pm
l1@x3441.6i	50,097	05/30/2000	2:04pm
L1@x3441.elem_min.txt	27,954	05/30/2000	2:43pm
L1@x3441.elem_tot.txt	27,967	05/30/2000	2:43pm
L1@x3441.elem_aqu.txt	29,627	05/30/2000	2:43pm
L00X3441.TXT	4,224	06/01/2000	12:16pm
L00x3441.bin	233,968	05/30/2000	2:36pm
l00x3441.6o	273,812	05/30/2000	2:36pm
L00x3441.6i	49,926	05/30/2000	2:10pm
l00x3441.6p	49,717	05/30/2000	2:36pm
L00x3441.elem_min.txt	2,092	05/30/2000	2:36pm
L00x3441.elem_tot.txt	2,105	05/30/2000	2:36pm

Table I-3. Contents of CD SLWBR3 (Continued)

File Name	File Size (bytes)	Date	Time
L00x3441.elem_aqu.txt	2,205	05/30/2000	2:36pm
L01X3441.TXT	16,857	06/01/2000	11:46am
l01x3441.6i	49,791	05/30/2000	3:10pm
L01x3441.bin	8,260,000	05/30/2000	4:02pm
l01x3441.6o	2,664,144	05/30/2000	4:02pm
l01x3441.6p	50,603	05/30/2000	4:02pm
L01x3441.elem_min.txt	24,422	05/30/2000	4:02pm
L01x3441.elem_tot.txt	24,435	05/30/2000	4:02pm
L01x3441.elem_aqu.txt	25,927	05/30/2000	4:02pm
L1AX4404.elem_aqu.txt	2,618	06/08/2000	12:22pm
L2AX4404.TXT	13,204	06/02/2000	5:34pm
L2AX4404.bin	94,781,104	06/08/2000	12:49pm
l2ax4404.6o	9,349,969	06/08/2000	12:49pm
l2ax4404.6i	35,567	06/08/2000	11:52am
l2ax4404.6p	36,191	06/08/2000	12:49pm
L2AX4404.elem_min.txt	71,032	06/08/2000	12:49pm
L2AX4404.elem_tot.txt	71,045	06/08/2000	12:49pm
L2AX4404.elem_aqu.txt	76,257	06/08/2000	12:49pm
L0B$4022.TXT	5,945	06/02/2000	5:37pm
L0B$4022.bin	40,341,376	06/08/2000	12:20pm
l0b$4022.6o	4,054,225	06/08/2000	12:20pm
l0b$4022.6p	46,731	06/08/2000	12:20pm
l0b$4022.6i	45,923	06/08/2000	11:54am
L0B$4022.elem_min.txt	32,122	06/08/2000	12:20pm
L0B$4022.elem_tot.txt	32,135	06/08/2000	12:20pm
L0B$4022.elem_aqu.txt	34,107	06/08/2000	12:20pm
l1ax4404.6tx	16,412	06/02/2000	10:48am
l1ax4404.6t	16,101	06/02/2000	10:48am
l2ax4404.6t	321,728	06/02/2000	12:15pm
l2ax4404.6tx	325,698	06/02/2000	12:15pm

Table I-4. Contents of CD SLWBR4

File Name	File Size (bytes)	Date	Time
L0@x1113.6i	50,237	04/12/2000	4:08pm
L0@X1113.TXT	27,265	05/08/2000	5:49pm
L0@x1113.bin	175,642,088	04/13/2000	2:31pm
l0@x1113.6o	15,838,820	04/13/2000	2:32pm
l0@x1113.6p	51,174	04/13/2000	2:32pm
L0@x1113.elem_min.txt	116,088	04/13/2000	2:31pm
L0@x1113.elem_tot.txt	116,101	04/13/2000	2:31pm
L0@x1113.elem_aqu.txt	123,089	04/13/2000	2:31pm
L1@X1113.TXT	39,255	05/08/2000	5:48pm
L1@x1113.bin	255,238,768	05/03/2000	7:41pm
l1@x1113.6i	40,725	05/03/2000	4:54pm
l1@x1113.6o	22,861,206	05/03/2000	7:42pm
l1@x1113.6p	40,153	05/03/2000	7:42pm
L1@x1113.elem_min.txt	155,403	05/03/2000	7:41pm
L1@x1113.elem_tot.txt	155,416	05/03/2000	7:41pm
L1@x1113.elem_aqu.txt	165,716	05/03/2000	7:41pm
L02g1113.bin	22,479,968	05/04/2000	5:26pm

Table I-4. Contents of CD SLWBR4 (Continued)

File Name	File Size (bytes)	Date	Time
L02G1113.TX0	44,330	05/19/2000	11:41am
L02G1113.TXT	4,323	05/08/2000	1:54pm
l02g1113.6o	2,351,383	05/04/2000	5:26pm
l02g1113.6i	39,831	05/04/2000	5:11pm
l02g1113.6p	39,905	05/04/2000	5:26pm
L02g1113.elem_min.txt	15,881	05/04/2000	5:26pm
L02g1113.elem_tot.txt	15,894	05/04/2000	5:26pm
L02g1113.elem_aqu.txt	16,954	05/04/2000	5:26pm
L02x1113.bin	22,566,216	05/04/2000	6:38pm
l02x1113.6o	2,395,199	05/04/2000	6:38pm
L02X1113.TXT	4,456	05/08/2000	6:02pm
l02x1113.6i	39,987	05/04/2000	4:58pm
l02x1113.6p	40,061	05/04/2000	6:38pm
L02x1113.elem_tot.txt	16,243	05/04/2000	6:38pm
L02x1113.elem_aqu.txt	17,327	05/04/2000	6:38pm
L02x1113.elem_min.txt	16,230	05/04/2000	6:38pm
l0ag2204.6o	2,802,953	03/14/2000	6:37pm
L0AG2204.TXT	84,647	04/24/2000	6:30pm
l0ag2204.6p	38,027	03/14/2000	6:37pm
L0Ag2204.6i	39,324	03/09/2000	9:34am
L0ag2204.bin	20,477,784	03/14/2000	6:37pm
L0ag2204.elem_min.txt	20,657	03/14/2000	6:37pm
L0ag2204.elem_tot.txt	20,670	03/14/2000	6:37pm
L0ag2204.elem_aqu.txt	22,162	03/14/2000	6:37pm
l0bg2022.6i	47,066	04/21/2000	11:37am
L0BG2022.TXT	7,229	05/08/2000	3:13pm
L0bg2022.bin	37,999,256	04/13/2000	12:22pm
l0bg2022.6o	4,812,437	04/13/2000	12:22pm
l0bg2022.6p	47,796	04/13/2000	12:22pm
L0bg2022.elem_min.txt	37,127	04/13/2000	12:22pm
L0bg2022.elem_tot.txt	37,140	04/13/2000	12:22pm
L0bg2022.elem_aqu.txt	39,424	04/13/2000	12:22pm
L0AO2204.TXT	94,529	04/24/2000	6:28pm
L0Ao2204.bin	31,970,656	03/14/2000	6:52pm
l0ao2204.6o	3,229,349	03/14/2000	6:52pm
l0ao2204.6p	40,996	03/14/2000	6:52pm
L0Ao2204.6i	40,191	03/09/2000	10:00am
L0Ao2204.elem_min.txt	25,192	03/14/2000	6:52pm
L0Ao2204.elem_tot.txt	25,205	03/14/2000	6:52pm
L0Ao2204.elem_aqu.txt	26,745	03/14/2000	6:52pm
l0Bo2022.6i	49,539	05/03/2000	5:04pm
L0BO2022.TXT	1,805	05/08/2000	8:57am
L0bo2022.bin	10,944,440	05/03/2000	6:18pm
l0bo2022.6o	1,859,726	05/03/2000	6:18pm

Table I-4. Contents of CD SLWBR4 (Continued)

File Name	File Size (bytes)	Date	Time
l0bo2022.6p	50,269	05/03/2000	6:18pm
L0bo2022.elem_min.txt	15,703	05/03/2000	6:18pm
L0bo2022.elem_tot.txt	15,716	05/03/2000	6:18pm
L0bo2022.elem_aqu.txt	16,608	05/03/2000	6:18pm
L1bo2022.bin	508,808	05/04/2000	5:21pm
L1BO2022.TXT	7,960	05/08/2000	8:56am
l1bo2022.6i	39,576	05/04/2000	5:13pm
l1bo2022.6o	227,275	05/04/2000	5:21pm
l1bo2022.6p	38,844	05/04/2000	5:21pm
L1bo2022.elem_min.txt	1,978	05/04/2000	5:21pm
L1bo2022.elem_tot.txt	1,991	05/04/2000	5:21pm
L1bo2022.elem_aqu.txt	2,091	05/04/2000	5:21pm

Table I-5. Contents of CD SLWBR5

File Name	File Size (bytes)	Date	Time
l01g1113.6o	28,394,929	05/04/2000	12:29pm
L01G1113.TXT	53,932	05/08/2000	1:56pm
L01g1113.bin	284,507,952	05/04/2000	12:29pm
l01g1113.6p	39,757	05/04/2000	12:29pm
l01g1113.6i	40,329	05/04/2000	10:53am
L01g1113.elem_min.txt	188,636	05/04/2000	12:29pm
L01g1113.elem_tot.txt	188,649	05/04/2000	12:29pm
L01g1113.elem_aqu.txt	201,589	05/04/2000	12:29pm
L01g2133.bin	283,227,992	05/04/2000	3:10pm
l01g2133.6i	38,726	05/03/2000	3:31pm
l01g2133.6o	28,302,025	05/04/2000	3:10pm
l01g2133.6p	38,242	05/04/2000	3:10pm
L01G2133.TXT	53,932	05/08/2000	6:29pm
L01g2133.elem_min.txt	181,485	05/04/2000	3:10pm
L01g2133.elem_tot.txt	181,498	05/04/2000	3:10pm
L01g2133.elem_aqu.txt	194,390	05/04/2000	3:10pm

Table I-6. Contents of CD SLWBR6

File Name	File Size (bytes)	Date	Time
L01g2133.bin	283,227,992	05/04/2000	3:10pm
l01g2133.6i	38,726	05/03/2000	3:31pm
l01g2133.6o	28,302,025	05/04/2000	3:10pm
l01g2133.6p	38,242	05/04/2000	3:10pm
L01G2133.TXT	53,932	05/08/2000	6:29pm
L01g2133.elem_min.txt	181,485	05/04/2000	3:10pm
L01g2133.elem_tot.txt	181,498	05/04/2000	3:10pm
L01g2133.elem_aqu.txt	194,390	05/04/2000	3:10pm
L01G4333.TXT	6,183	06/01/2000	10:04am
L01g4333.bin	34,842,248	05/31/2000	5:17pm
l01g4333.6i	38,538	05/31/2000	5:07pm
l01g4333.6o	3,073,462	05/31/2000	5:17pm
l01g4333.6p	38,122	05/31/2000	5:17pm
L01g4333.elem_min.txt	22,163	05/31/2000	5:17pm
L01g4333.elem_tot.txt	22,176	05/31/2000	5:17pm
L01g4333.elem_aqu.txt	23,668	05/31/2000	5:17pm
L01x1113.bin	284,828,024	05/04/2000	1:28pm
L01X1113.TXT	53,932	05/08/2000	6:01pm
l01x1113.6o	28,446,830	05/04/2000	1:29pm
l01x1113.6i	40,403	05/04/2000	10:37am
l01x1113.6p	39,913	05/04/2000	1:29pm
L01x1113.elem_min.txt	188,287	05/04/2000	1:28pm
L01x1113.elem_tot.txt	188,300	05/04/2000	1:28pm
L01x1113.elem_aqu.txt	201,216	05/04/2000	1:28pm

Table I-7. Contents of CD SLWBR7

File Name	File Size (bytes)	Date	Time
l02g2133.6i	38,542	03/20/2000	4:52pm
l02g2133.6o	29,453,749	03/20/2000	6:49pm
l02g2133.6p	38,538	03/20/2000	6:49pm
L02G2133.TXT	56,060	03/27/2000	2:35pm
L02g2133.elem_min.txt	188,899	03/20/2000	6:48pm
L02g2133.elem_tot.txt	188,912	03/20/2000	6:48pm
L02g2133.elem_aqu.txt	202,332	03/20/2000	6:48pm
L02G4333.TXT	10,306	06/01/2000	10:16am
L02g4333.bin	58,376,792	05/31/2000	6:11pm
l02g4333.6o	5,133,306	05/31/2000	6:11pm
l02g4333.6i	38,270	05/31/2000	5:54pm
l02g4333.6p	38,336	05/31/2000	6:11pm
L02g4333.elem_min.txt	37,170	05/31/2000	6:11pm
L02g4333.elem_tot.txt	37,183	05/31/2000	6:11pm
L02g4333.elem_aqu.txt	39,707	05/31/2000	6:11pm
L0An2204.bin	131,050,544	03/08/2000	4:42pm
L0AN2204.TXT	540,056	04/24/2000	6:26pm
L0An2204.6i	37,817	03/08/2000	3:51pm
L0An2204.elem_min.txt	96,382	03/08/2000	4:42pm

Table I-7. Contents of CD SLWBR7 (Continued)

File Name	File Size (bytes)	Date	Time
L0An2204.elem_tot.txt	96,395	03/08/2000	4:42pm
L0An2204.elem_aqu.txt	103,479	03/08/2000	4:42pm
L0AX1203.TXT	160,598	04/24/2000	6:29pm
L0ax1203.bin	38,921,928	03/04/2000	5:54pm
L0Ax1203.6i	39,323	03/04/2000	3:08pm
L0ax1203.elem_min.txt	33,007	03/04/2000	5:54pm
L0ax1203.elem_tot.txt	33,020	03/04/2000	5:54pm
L0ax1203.elem_aqu.txt	35,424	03/04/2000	5:54pm
L0ax2204.bin	131,014,704	05/15/2000	6:25pm
L0AX2204.TXT	16,271	05/16/2000	3:01pm
L0Ax2204.6i	39,351	03/08/2000	1:15pm
L0AX2204.TXU	16,271	05/11/2000	3:40pm
l0ax2204.6o	14,516,620	05/15/2000	6:25pm
l0ax2204.6p	38,281	05/15/2000	6:25pm
L0ax2204.elem_min.txt	94,107	05/15/2000	6:25pm
L0ax2204.elem_tot.txt	94,120	05/15/2000	6:25pm
L0ax2204.elem_aqu.txt	101,036	05/15/2000	6:25pm
L0b$2022.bin	33,741,192	05/16/2000	1:29pm
l0b$2022.txt	5,917	05/16/2000	3:04pm
l0b$2022.6i	46,396	04/12/2000	4:09pm
l0b$2022.6o	4,052,187	05/16/2000	1:29pm
l0b$2022.6p	47,426	05/16/2000	1:29pm
L0b$2022.elem_min.txt	30,967	05/16/2000	1:29pm
L0b$2022.elem_tot.txt	30,980	05/16/2000	1:29pm
L0b$2022.elem_aqu.txt	32,880	05/16/2000	1:29pm
l0bn2022.6i	45,125	04/12/2000	4:12pm
L1ag2204.elem_min.txt	66,807	03/23/2000	11:38am
L1ag2204.elem_tot.txt	66,820	03/23/2000	11:38am
L1ag2204.elem_aqu.txt	71,720	03/23/2000	11:38am
L1AG2204.TXT	11,685	04/21/2000	12:04pm
L1ag2204.bin	94,928,056	03/23/2000	11:38am

Table I-8. Contents of CD SLWBR8

File Name	File Size (bytes)	Date	Time
L00.bat	3,696	05/03/2000	5:07pm
L001.bat	704	06/08/2000	11:48am
L006.bat	1,058	04/21/2000	11:31am
L00G4333.TXT	80,287	06/01/2000	10:27am
L00G4333.TX0	280,020	06/07/2000	1:39pm
L00g4333.6i	50,283	05/30/2000	10:46am
L00g4333.bin	338,855,936	05/30/2000	12:53pm
l00g4333.6o	28,939,785	05/30/2000	12:53pm
l00g4333.6p	50,516	05/30/2000	12:53pm
L00g4333.elem_min.txt	222,312	05/30/2000	12:53pm
L00g4333.elem_tot.txt	222,325	05/30/2000	12:53pm
L00g4333.elem_aqu.txt	236,153	05/30/2000	12:53pm
L1ax2204.bin	84,451,160	05/15/2000	6:58pm
l1ax2204.6i	35,613	05/15/2000	6:41pm
l1ax2204.6o	9,169,078	05/15/2000	6:58pm
l1ax2204.6p	35,433	05/15/2000	6:58pm
l1ax2204.txt	8,995	05/16/2000	3:03pm
L1ax2204.elem_min.txt	59,982	05/15/2000	6:58pm
L1ax2204.elem_tot.txt	59,995	05/15/2000	6:58pm
L1ax2204.elem_aqu.txt	64,391	05/15/2000	6:58pm
l2bo2022.6i	38,918	05/05/2000	12:19pm
L2BO2022.TXT	5,816	05/08/2000	8:59am
L2bo2022.bin	35,518,880	05/05/2000	2:33pm
l2bo2022.6o	3,426,482	05/05/2000	2:33pm
l2bo2022.6p	38,746	05/05/2000	2:33pm
L2bo2022.elem_min.txt	24,721	05/05/2000	2:33pm
L2bo2022.elem_tot.txt	24,734	05/05/2000	2:33pm
L2bo2022.elem_aqu.txt	26,346	05/05/2000	2:33pm

Table I-9. Contents of CD SLWBR9

File Name	File Size (bytes)	Date	Time
PP User's Manual.doc	1,084,416	01/25/2000	11:11pm
User request for PP.doc	43,520	01/26/2000	9:09am
Sea.tmp	669	12/22/1999	2:02pm
TEMPLATE.TMP	579	12/15/1999	3:21pm
atwts.in	1,020	07/06/1999	3:13pm
data.in	1,772	01/06/2000	7:37pm
eqsetup.c	42,392	07/07/1999	11:27am
eqsetup.exe	237,620	10/19/1999	4:28pm
junk.out	0	01/06/2000	7:44pm
LWBRjunk.txt	3,698	10/20/1999	11:20am
ratefacs.in	96	10/20/1999	10:16am
template.in	50,803	11/11/1999	9:01pm
Data0.nuc	2,305,995	05/16/2000	12:17pm
data0.ymp	2,710,251	06/07/2000	3:29pm
Data0criticaliy.txt	2,305,995	05/16/2000	12:13pm
data0.nuc.R8d.Th2	2,304,555	10/19/1999	5:16pm
data0.ymp.R0A.SRL	2,706,244	05/25/2000	10:00am
data1.nuc	795,838	05/16/2000	1:16pm
data1.ymp	792,180	06/07/2000	3:29pm
data1f.nuc	928,097	05/16/2000	1:16pm
slist.nuc	60,392	05/16/2000	1:16pm
slist.ymp	57,434	06/07/2000	3:29pm
output.nuc	50,613	05/16/2000	1:16pm
output.ymp	46,807	06/07/2000	3:26pm
SQR_eq6new.doc	2,641,408	12/23/1998	12:51pm
EQ_I_PC.DOC	97,792	07/09/1998	12:29pm
L0ax2204.bin	131,192,784	03/08/2000	1:46pm
L0AX2204.TXT	540,056	04/24/2000	6:27pm
L0ax2204.elem_tot.txt	98,020	03/08/2000	1:46pm
L0ax2204.elem_aqu.txt	105,224	03/08/2000	1:46pm
L0ax2204.elem_min.txt	98,007	03/08/2000	1:46pm
L0b$2022.bin	37,230,760	04/13/2000	1:08pm
L0B$2022.TXT	616,503	05/10/2000	6:37pm
l0b$2022.6o	4,441,114	04/13/2000	1:08pm
l0b$2022.6p	47,130	04/13/2000	1:08pm
L0b$2022.elem_tot.txt	34,060	04/13/2000	1:08pm
L0b$2022.elem_min.txt	34,047	04/13/2000	1:08pm
L0b$2022.elem_aqu.txt	36,152	04/13/2000	1:08pm
data1f.ymp	925,280	06/07/2000	3:29pm
Excel	5,070,336	08/30/2000	7:01pm
PP.exe	308,609	10/10/1998	4:15pm
PREFER.PP	66	06/07/2000	1:44pm

Contents of Directory "Excel" on CD SLWBR9

File Name	Calculations	File Size (bytes)	Date	Time
LWBRshipGdThU.xls	Gd, Th, and U loss from WP	4,364,800	08/30/2000	7:00pm
ShipLWBR.xls	Al fill density (ρ), volume (V), moles, surface area (SA); Convert degradation rates of Al fill, steels, and SNF to mol/cm^2·sec; Convert compositions of Al fill and SNF to moles/100g for EQ6	97,792	08/30/2000	6:16pm
A516_Rate.xls	A516 carbon steel degradation rates	20,480	08/30/2000	10:07am
density_LWBR.xls	WP corrosion products ρ and mass	240,640	08/30/2000	6:10pm
doecan_EDA2.xls	V, SA, molar volume and 100g-moles of WP components; Void space in WP	79,360	08/30/2000	6:15pm
Glass_rates_110999.xls	HLW glass degradation rates	30,208	08/30/2000	1:49pm
HLW_glass.xls	100g-mole and simplified HLW glass compositions and degradation rates	72,704	08/30/2000	5:36pm
LWBRj13evaporIIK3.xls	Concentration of salts evaporated from J-13 water	34,816	08/30/2000	6:40pm
LWBR_gd_conc_needed_for_loss.xls	Gd loss from WP as a function of pH and J-13 water flushing rates	53,760	08/30/2000	6:26pm
LWBRshapes.xls	ρ of SNF; Number of SNF pellets in rods of SNF assemblies; Total dimensions, V, SA, and mass of AM350 grids	75,776	11/09/1999	4:00pm

OFFICE OF CIVILIAN RADIOACTIVE WASTE MANAGEMENT
SPECIAL INSTRUCTION SHEET

1. QA: QA

Complete Only Applicable Items

This is a placeholder page for records that cannot be scanned or microfilmed

2. Record Date	3. Accession Number
09/14/2000	ATT-TO MOL. 20000926.0295
4. Author Name(s)	**5. Author Organization**
SARA ARTHUR	N/A

6. Title
EQ6 CALCULATION FOR CHEMICAL DEGRADATION OF SHIPPINGPORT LWBR (TH/U OXIDE) SPENT NUCLEAR FUEL WASTE PACKAGES

7. Document Number(s)	8. Version
CAL-EDC-MD-000008	REV. 00

9. Document Type	10. Medium
~~CD-ROM~~ DATA	~~DATA~~ OPTICAL DISK

11. Access Control Code
PUB

12. Traceability Designator
DC #24931

13. Comments
THIS IS A SPECIAL PROCESS CD-ROM, (ATTACHMENT II 9-CD'S), AND CAN BE LOCATED THROUGH THE RPC